Environmental Chemistry Letters (2021) 19:2551–2579
https://doi.org/10.1007/s10311-020-01168-6

REVIEW

Indoor formaldehyde removal by catalytic oxidation, adsorption and nanofibrous membranes: a review

Berly Robert[1] · **Gobi Nallathambi**[1]

Received: 23 November 2020 / Accepted: 18 December 2020 / Published online: 21 January 2021

Abstract

Indoor pollution of air by formaldehyde poses a serious threat to human health because formaldehyde causes illnesses and discomfort even at low levels, thus calling for abatement techniques. Techniques include absorption, physisorption, chemisorption, biological and botanical filtration, photocatalytic decomposition, membrane separation, plasma and catalytic oxidation. Here we review the principles, performances, advantages and disadvantages of these techniques, with focus on catalytic oxidation, adsorption and the use of nanofibrous membranes. Supported noble metal and metal oxide-based materials are efficient catalysts for oxidation. We present photocatalytic oxidation under UV, visible and solar light using composites. Chemisorption method is reviewed with focus on amino-containing adsorbents, conditions of temperature and relative humidity and surface properties. Nanofibrous membranes display high density of active sites for pollutant interactions and allow formaldehyde removal without leaching out of catalyst nanoparticles or adsorbents.

Keywords Air quality · Air remediation · Filtration · Formaldehyde removal · Photocatalysis · Catalytic oxidation · Nanomaterials · Adsorption · Nanofibrous membrane

Abbreviations

FTIR	Fourier transform infrared spectroscopy
ppm	Parts per million
VOC	Volatile organic compound
TiO_2	Titanium dioxide
H_2O	Water
CuO	Copper oxide
HCHO	Formaldehyde
Ce_2O	Cerium oxide
CO_2	Carbon dioxide
ZnO	Zinc oxide
NO_x	Nitrogen oxides
WO_3	Tungsten trioxide
Cu-Ce	Copper-Ceria
ZnS	Zinc sulphide
N_2	Nitrogen
Bi	Bismuth
CdS	Cadmium sulphide
Ag	Silver
PbS	Lead sulphide
h^+	Holes
NiO	Nickel oxide
E^-	Electrons
Fe_2O_3	Iron(III) oxide
$OH^\bullet$	Hydroxyl radicals
SnO_2	Tin oxide
Fe	Iron:
MnO_2	Manganese dioxide
Au	Gold
$O^{2\bullet-}$	Superoide radical anion
C	Carbon
Mn	Manganese
S	Sulphur
Cr	Chromium
Cu	Copper
Ru	Ruthenium
ZIF-8	Zeolitic imidazolate framework-8
La	Lanthanum
MIL	Material from Institute Lavoisier
Pr	Praseodymium
$MgAl_2O$	Magnesium aluminate
Pt	Platinum

✉ Gobi Nallathambi
gobsnn@gmail.com

[1] Department of Textile Technology, Anna University, Chennai 600 025, India

$MgTiO_3$	Magnesium titanate
NH_2	Amino group
2-CEES	2-Chloroethyl ethyl sulphide
MOF	Metal–organic frameworks
Cu	Copper
Ti_8O_8	Titanium-based clusters
Co	Cobalt
Xe	Xenon
GHSV	Gas hourly space velocity
$MnCo_3$	Manganese carbonate
MBTH	3-Methyl-2-benzothiazolinone hydrazone
MnO_2	Manganese dioxide
$Co_xMn_{3-x}O_4$	Cobalt manganese oxide
rGO/TiO_2	Titanium dioxide nanoparticles immobilized on reduced graphene oxide
α-MnO_2@L-MnO_2	Growth of layered manganese dioxide nanosheets over α-MnO2 nanotubes
Pt/ZSM-5	Zeolite Socony Mobil-5-supported Platinum
Bi_2O_3/TiO_2	Titanium dioxide doped with Bismuth trioxide
C_6H_6	Benzene
LED	Light-emitting diode
$CH_3COOCH_2CH_3$	Ethyl acetate
ppbv	Parts per billion volume
Bi_2MoO_6	Bismuth molybdenum oxide
g-C_3N_4	Graphitic carbon nitride
MnO_2-CF	Manganese dioxide/carbon foam composite
AlOOH	Aluminium oxyhydroxides
ACS-O	Preoxidized activated carbon spheres
Ga_2O_3	Gallium oxide
Ir_xPt_{1-x}/Nb_2O_5	Niobium oxide nanoparticle-supported platinum-iridium bimetallic nanocatalysts
TMSPDETA	N1-(3-(trimethoxysilyl)-propyl) diethylenetriamine
APTES	3-Aminopropyl- triethoxysilane
MCM-41	Mesoporous Silica—mobil composition of matter No. 41
AEAPMDMS	G-Aminopropylmethyl dimethoxysilane
HMDA	Hexamethylene diamine
SBA-15	Silica mesoporous—Santa barbara amorphous-15
GC/FID	Gas chromatography–flame ionization detection
US EPA	United states environmental protection agency
THF	Tetrahydrofuran
G-GND/S	Graphene sponge decorated with graphene nanodots
DMF	Dimethylformamide
DETA	Diethylenetriamine
DI	Deionized water
$Si_{12}Mg_8O_{30}(OH)_4(OH_2)_4 .8H_2O$	Sepiolite a hydrated magnesium silicate
BET	Brunauer–Emmett–TellerDMSO Dimethyl
PMMA@PDA	Polydopamine-coated polymethyl methacrylate electrospun-fiber
ppmv	Parts per million by volume
NH_3	Ammonia

Introduction

Nowadays, a major challenge is the indoor air quality and to keep indoor air pollutants at lowest exposure levels possible, to minimize its adverse effects on both air quality and human health. Most indoor living facilities emit organic or inorganic pollutants, particulate matter and aerobes. The most frequently detected volatile organic compound (VOC) and the primary ubiquitous indoor air pollutant that causes mild-to-chronic effects in humans is formaldehyde. They are large group of carbon-based chemicals that easily evaporate at room temperature and has been classified as carcinogenic to humans in 2004 (Salthammer et al. 2010). However, formaldehyde-based chemistry serves a number of purposes by itself or in combination with other chemicals. For example, it is used in manufacture of resins like urea–formaldehyde, dyes like indigo and para-rosaline, used in processing of anti-polio vaccine, used as decolorizing agent in vat dyes, 30–50% aqueous solution of formaldehyde stabilized in certain percentage of methanol called as formalin is used as disinfectant, germicide and fungicide, and historically it has been used to impart permanent set to clothing, e.g. pleats in wool skirts (Gard 1957; Mugal et al. 2013).

Studies have confirmed that the level of formaldehyde is significantly higher, indoors than in outdoor environments (Lee et al. 2018). This is because within the small indoor boundaries we have many sources of formaldehyde like construction materials, carpets, other fabrics, adhesives, paints and coatings, lacquers, finishes, wall papers, scented products, cosmetics, cigarette smoke, wood smoke and fuel burning appliances like gas stoves (Kelly et al. 1999; An et al. 2010). Formaldehyde can be released into the air continuously for months to several years from adhesives like urea–formaldehyde resins that are being used in interior

decorative materials. In general, formaldehyde exposure levels are highest when the products are new, and when the temperature and humidity indoors are very high. In such cases, the immediate solution to reduce the formaldehyde emission would be to increase the ventilation rate in the room; however opening windows and ventilating the room is not possible in a polluted city (Miao et al. 2019), control the humidity, maintain a moderate temperature by using dehumidifiers and air conditioning systems or plan an intelligent housing construction and use of wooden pieces or products that have been off-gassed.

According to World Health Organization, the formaldehyde concentration indoor should not exceed 0.1 mg/m^3 and according to the Agency for Toxic Substances and Disease Registry, levels from 0.4 to 3 ppm can produce symptoms of mild to moderate irritation of the eyes, nose, throat and many other diseases. Higher levels have been linked to increased risk of some cancer types. Moreover, since humans spend 80–90% of their life indoors (home, office, cars or shopping malls), it has become very important in developing solutions for clean indoor-air, along with abatement of indoor formaldehyde emission rates at low temperature, especially at room temperature. So far, multiple approaches have been investigated to improve the air quality and for lowering the concentration of indoor formaldehyde, including adsorption, plasma decomposition with or without the assistance of catalyst, thermal oxidation, catalytic oxidation, photocatalytic oxidation, biological/botanical filtration, e.g. phytoremediation and microbial removal (Berly and Nallathambi 2020; Suresh and Bandosz 2018; Guo et al. 2019; Pei and Zhang 2011; Torees et al. 2013; Shah and Li 2019; Indarto et al. 2008). Apart from these major methods for formaldehyde removal, there is membrane technology that will implement one of the above or a combination of above methods into one single membrane contributing to volatile organic compounds (VOC) abatement methods. There are two broad approaches to these formaldehyde removal methods, (i) recovery and (ii) destruction. Adsorption, absorption, condensation and membrane separation techniques fall under recovery method (Fig. 1). Whereas, plasma decomposition, thermal and non-thermal catalytic oxidation, photocatalytic oxidation, biological/botanical filtration and incineration fall under the destructive method, wherein the formaldehyde is converted into benign, odourless and environmentally friendly components like H_2O and CO_2 (Zhang et al. 2017; Na et al. 2018).

Unlike photocatalytic oxidation, which is effective at higher pollutant concentration levels, plasma or non-thermal plasma (cold oxidation) technology can be very effective even at lower VOC concentration. This method disassociates the VOCs into carbon dioxide and water using radicals (plasma-cluster ions) created by air ionizers (Sultana et al.

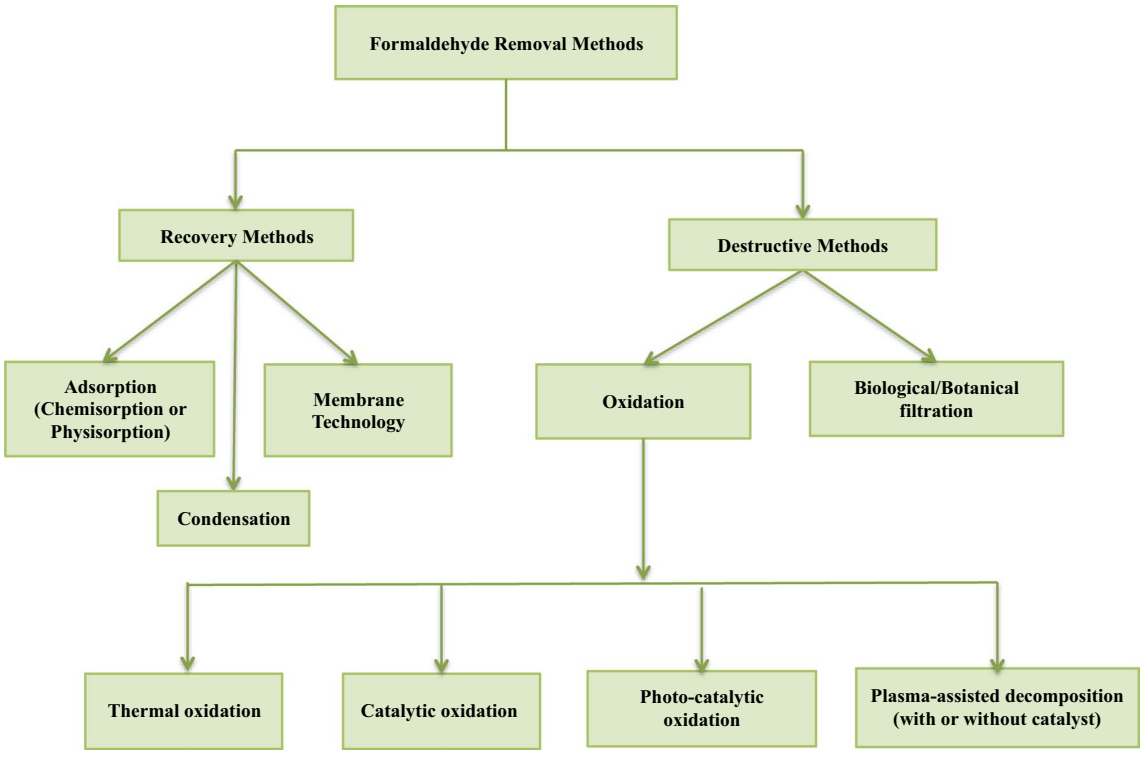

Fig. 1 Methods for removal of volatile organic compounds (VOC) from air. Recovery and destruction are the two broad approaches to these formaldehyde or any VOC removal methods

2015; Lu et al. 2012). The main disadvantage of using this air cleaning technology to remove toxic volatile contaminants in air is the possible generation of harmful byproducts, and release of significant amount of ozone and NO_x, causing secondary pollution. Research was conducted to study the efficacy of plasma and catalytic oxidation combined together for formaldehyde removal (Pei and Zhang 2011). Zhu et al. (2015) studied the plasma-catalytic oxidation of formaldehyde through a coaxial dielectric barrier discharge reactor over a series of Cu–Ce oxide catalysts prepared by the citric acid sol–gel method. In comparison with the plasma-only process, plasma combined with catalytic oxidation was quite effective in enhancing the usual reaction performance. The surface-adsorbed oxygen species were increased with the Cu and Ce interaction, facilitating the redox cycles, which significantly increased the formaldehyde removal efficiency.

Kim et al. (2010) studied the potential of phytoremediation in formaldehyde removal using 86 species of plants, by exposing the plants to gaseous formaldehyde in a closed chamber. Among ferns, woody foliage plants, herbaceous foliage plants, Korean native plants and herbs, ferns had the highest formaldehyde removal efficiency. In general, some plants can absorb and metabolize VOCs. Han and Ruan (2020) have done a comprehensive and systematic review on the effect of indoor plants on air quality. In spite of the fact that the easiest method, phytoremediation could be comparatively cheaper than all the formaldehyde removal methods, it is still not considered as an effective method as it takes a very long time to observe the actual effect (Yang et al. 2020).

Another slight variation to this method is the biological filtration, which uses microorganisms or biologically active materials, primarily based on compost or soil, to vent out the environmentally undesirable compounds, e.g. VOCs and air toxins. This biological component was mainly used in wastewater treatment but later was considered for the removal of pollutants from air as well. Open single-bed, multiple story or stacked bed systems are the common installation types of these bio-filters. It mainly consists of bio-film or biologically active layer, which induces an aerobic degradation reaction to metabolize the target pollutants giving raise to harmless CO_2, H_2O and some microbial biomass as end products (Leson and Winer 1991; Guieysse et al. 2008). Yuxia et al. in 2019 developed an efficient plant–microbe phytoremediation method using three plant species and adding cultured microorganism into their rhizosphere (narrow portion of soil-area around plant root). Compared to plant-only system without the addition of microorganisms, the plant–microbe system showed far greater removal efficiency for formaldehyde removal (Yang et al. 2020). However, there exist many unanswered queries with regard to botanical/biological filtration, like microbial decomposition kinetics, its effectiveness under normal room conditions, degradation rate as induced by the microbes, and if the degradation rate is adequate for a significant amount of formaldehyde removal over time (Pei and Zang 2011).

Absorption method is another simple technology considered for VOC abatement, mainly for the treatment of industrial gaseous effluents by dissolving the pollutant into a liquid solvent. The choice of suitable solvent system/liquid absorbent is the fundamental variable. Normally, the common absorbent used is water or aqueous solutions using bases, acids or oxidizing reagents. In the case of aromatic and aliphatic hydrocarbons or hydrophobic VOCs like xylene, toluene, benzene and so on, alternate solvent system has to be considered, such as high-boiling absorbents, water–solid suspensions or water–oil emulsions (Heymes et al. 2006). For example, polyglycols and silicone oil (polydimethylsiloxane an oil-based absorbent) were used for hydrophobic VOCs absorption (Guillerm et al. 2017; Chiang et al. 2012). Fatima et al. (2020) synthesized bio-based ionic liquids obtained from environmentally friendly chemicals as starting materials for absorbing the VOCs. Solvent degradation, regeneration of used solvent or equipment corrosion is the major disadvantages of using this technique.

The membrane-based recovery is a process that has been used back in 1960 for desalination purposes. Membrane materials can be polymeric, inorganic or a combination of both. In the year 1987, some researchers conducted air and vapour permeation experiments on various membranes including neoprene and nitrile rubber, polyvinyl chloride, silicone polycarbonate, hypalon and fluorel membranes. Of these materials, silicone rubber and neoprene membranes can be made easily (Baker et al. 1987). However, to some organic vapours like gasoline, the resistance of silicon rubber is quite poor. Hence researchers have been exploring polymeric materials with high organic resistance. For this purpose, Deng et al. (1995) investigated asymmetric aromatic polyimide membranes prepared by the phase-inversion technique, which are found to be very effective in removing gasoline vapours and other VOCs too from the air. Although the membrane-based separation can be an effective VOC removal approach, its adaptability is questionable because of multiple factors like adaptability to range of organics, cost and maintenance of membrane, the process rate (it is directly proportional to operating cost), re-chargeability or re-usability of membranes (Khan and Ghoshal 2000). Zeolite (crystalline aluminosilicate minerals) and silica membranes are considered as inorganic membranes having high permeability, tunable selectivity, high thermal and chemical resistance (Aguado et al. 2004; Jang et al. 2011). Jang et al. (2011) fabricated continuous mesoporous silica membranes on polymeric hollow fibres for gas separation. The synthesized membranes have high gas flux and the surface can be modified (for example functionalized by inclusion of an amine) to drastically improve selectivity. Hence, such

membranes can also be considered for formaldehyde or any VOC removal.

Formaldehyde can also be removed using condensation method by lowering the temperature of gas stream containing the VOCs using N_2 at cryogenic temperatures or by increasing pressure (Aguado et al. 2004). This cryogenic condensation technique uses liquid N_2 by exploiting the vapour–liquid equilibrium principle of multi-component mixtures and is mostly considered in companies and industries to comply with the emission standards. Proper disposal of the spent coolant is one of the drawbacks of condensation process. However, when dealing with indoor formaldehyde levels (which are usually within the ppm or sub-ppm levels) catalytic oxidation and adsorption (especially chemisorption) are shown to be more effective in controlling VOCs and will be discussed in this review in detail.

Formaldehyde removal by oxidation

One of the most mature, since the 1940s, and effective technologies for VOC removal is the use of an oxidation system, a chemical conversion process, applicable for different kinds of pollutants, which can oxidize the VOCs into benign, odourless and environmentally friendly components like CO_2, H_2O and various oxides. Basically the oxidation technique of formaldehyde removal is categorized into photocatalytic oxidation, catalytic oxidation and thermal oxidation.

Photocatalytic oxidation

The technique of photocatalytic oxidation uses solids such as nano-semiconductor catalysts that can promote reactions at ambient temperature, in the presence of ultraviolet light without being consumed in the overall reaction involving conversion of organic or inorganic compounds into harmless and odourless constituents. It is obvious that photodegradation of formaldehyde depends strongly on ultraviolet light-illumination (with a wavelength below 388 nm) or photon flux on the catalyst surface. The commonly used artificial light sources (ultraviolet lamps) include mercury vapour lamps, black-light lamps and ultraviolet lasers. However, these lamps are fragile, produce unstable output power, are highly toxic and the life span of these light sources are quite short. Conversely, light-emitting diodes (semiconductor-based lighting devices) have a longer life with low electricity consumption, do not contain toxic mercury and are highly reliable (Levine et al. 2011; Shie et al. 2008).

The most extensively used photocatalyst is TiO_2, since it has found to have the most appealing and superior properties such as it is inexpensive, non-toxic, chemically inert, photo-stable and easy to activate under ultraviolet or near ultraviolet light. Apart from TiO_2, some good number of other compounds like CuO, Ce_2O, ZnO, WO_3, ZnS, CdS, PbS, NiO, Fe_2O_3, SnO_2, MnO_2, Bi-based, Ag-based and few others having ample band-gap energies are also found to be promoting the photocatalytic activity (Lin et al. 2012; Talaiekhozani et al. 2020). However, CdS and PbS (both binary metal sulphide semiconductors) are considered toxic and are not stable for catalysis. Though WO_3 is identified as a promising photocatalyst, its activity is not as good as TiO_2 in comparison, but are effective when used along with other semiconductors including TiO_2 (Ibhadon et al. 2013). Similarly, even though ZnO shows a good photocatalytic activity in aqueous-phase compared to TiO_2, the stability of ZnO is not as good as TiO_2 (Talaiekhozani et al. 2020). The basic mechanism of pollutant degradation through photocatalytic oxidation is shown in Fig. 2.

Sun et al. (2010) studied photocatalytic oxidation of formaldehyde on the TiO_2 under dry and humid conditions. It is through H-bonding, the formaldehyde is adsorbed on hydroxyl groups of catalyst surface. Here humidity plays a positive role, as with the presence of some water, there is an accumulation of hydroxyl radical (powerful oxidant due to its high redox potential) on the catalyst surface. Consequently, formation of formate species (intermediate compound) and the final products CO_2 and H_2O are increased significantly. As a matter of fact, TiO_2 is an effective photocatalyst, which exhibits high activity only under the ultraviolet light range, making it unsuitable for its usage in indoor applications or inside vehicles. Hence, in the recent past the traditional photocatalytic oxidation has been modified with the use of catalysts that will show photocatalytic activity under visible illumination. This capability of a catalyst to absorb visible wavelength is possible only by considering certain critical factors and by altering the band gap of the catalysts that have been used as photocatalyst. For example, TiO_2 can be doped with transition metal ions (Mn, Cr and so on), with Ag, Ru, Fe, Au and with non-metal species (C, N, S), thus reducing band gap energy and demonstrating a red-shift in catalyst absorption band from ultraviolet region to the visible region (Basavarajappa et al. 2020; Klauson et al. 2008; Louangsouphom et al. 2019). However, the formaldehyde removal efficiency by photocatalytic oxidation remains quite low especially with the visible light active silver/nitrogen/tungsten-doped photocatalysts (Luna et al. 2018; Liu et al. 2006; Lin et al. 2012). Moreover, they are known to be effective in higher VOCs concentration and generate secondary pollutants as well. The VOC conversion or the degradation rate decreases drastically when the VOC levels drop below 1 ppm.

The combination of photocatalytic technology with adsorption technology is found to be an attractive alternative and was investigated by many researchers. This adsorbent-photocatalyst hybrid was developed with main intension to address the high aggregation tendency of TiO_2 or any other

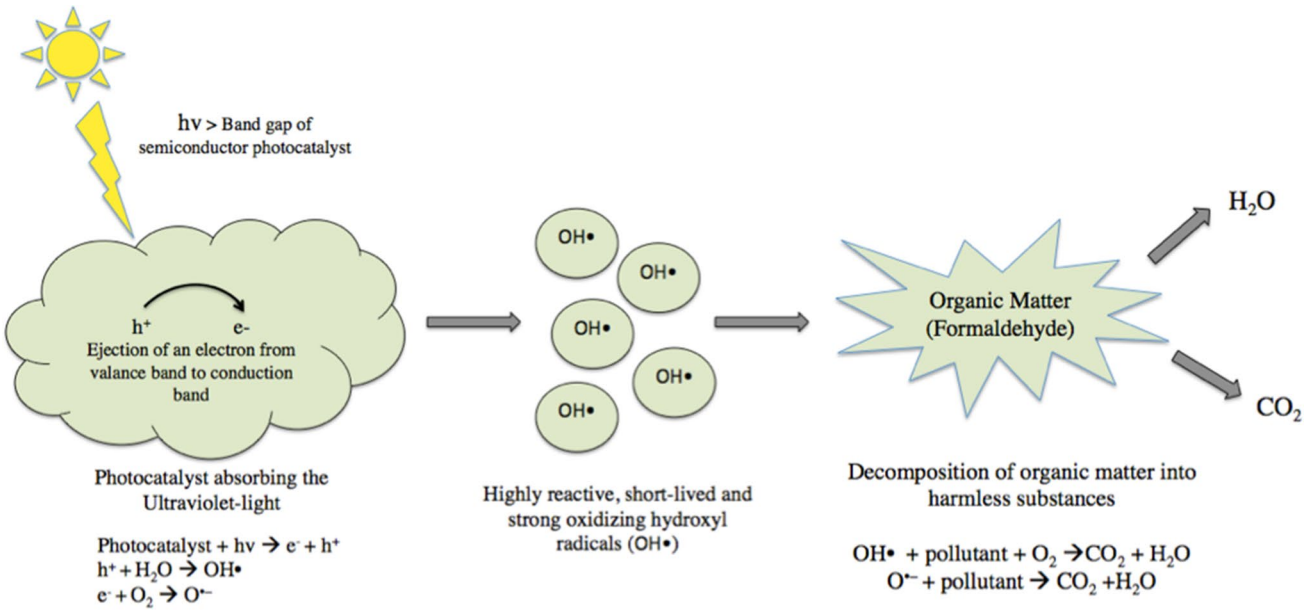

Fig. 2 Mechanism of photocatalytic oxidation. Photocatalysis takes place when light/photon with energy hν (where h is Planck's constant, ν is frequency) is absorbed by catalyst particle. This happens only when hν is greater than or equivalent to band gap energy of photocatalyst, resulting in ejection of electron (e^-) from valence band to conduction band. The holes (h^+) that are left in valence band of photocatalyst can react with water molecules to generate hydroxyl radicals (OH•). These radicals are responsible for the degradation of organic pollutants to carbon dioxide (CO_2) and water (H_2O), as they have strong oxidizing power. At the same time, electrons in conduction band can react with oxygen species and form highly reactive intermediate species with high-standard redox potentials called the superoxide radical anion ($O_2^{\bullet-}$). These can then mineralize organic substrates to CO_2 and H_2O

photocatalytic nanoparticles. With agglomeration, there is a very low utilization of active sites present in photocatalyst, leading to poor absorption of pollutants and low photocatalytic activity. Hence, a strategy to immobilize or disperse the photocatalytic material on certain matrix or porous material (an adsorbent like activated carbon or metal–organic frameworks) with high surface area was looked into. Lu et al. (2010) investigated removal of indoor low-concentration formaldehyde (initial concentration below 1 ppmv) using TiO_2 films coated on activated carbon filters and on glass plate. It was concluded that nanosized TiO_2 particles immobilized on the surface of activated carbon filter performed better (with formaldehyde removal of 79.4%) than TiO_2 film coated on glass (with formaldehyde removal of 25.7% only). Apart from activated carbon, few other supports for photocatalytic materials have been investigated, including zeolites, glass, polymeric materials, graphene, natural silicates, MOFs and other porous molecular sieves. Besides, TiO_2 often suffers from recombination of charge carriers (photo-induced electron–hole pairs). Doping of heteroatoms into TiO_2 lattice can perhaps prevent the recombination of charge carriers by narrowing down its band gap (Liu D et al. 2020).

In addition, the coupling of photocatalyst with metal–organic frameworks (MOF: another special class of porous materials)-based adsorbents might be a very good route for the application of photocatalytic technology for indoor formaldehyde (at a concentration level below 1 ppmv) removal. Due to MOF's tunable pore size, large pore volume, adjustable chemistry, semiconductors like properties and mesopores supplying a larger specific surface area, it has been considered for a wide range of applications. Huang et al. (2019) investigated and synthesized TiO_2@NH_2-MIL-125 (using a simple in-situ solvothermal method) composite photocatalysts for formaldehyde removal under ultraviolet irradiation by offering more adsorption sites and facilitating mass transfer. Basically, NH_2-MIL-125 is a MOF made of Ti_8O_8 ring-shaped metal cluster linked by terepthalate and contains NH_2 functional moieties. These are relatively inexpensive, non-toxic, water/photo-stable and also bring in ancillary advantages in adsorption and catalysis. High dispersion of TiO_2 particles on the surface of NH_2-MIL-125, and a strong electronic interaction (Ti–N–C) between elements of the composite was evident from their results. Ren et al. (2020) in the year prepared a class of novel MOF, Zeolitic imidazolate framework-8 (ZIF-8) assembled on TiO_2-coated activated carbon fibre felts to achieve a highly efficient removal of formaldehyde under ultraviolet light. ZIF-8 is considered as an excellent adsorbent material due to their robust porosity (diameters of within 2.0 nm), exhibiting strong van der waals forces for effective adsorption of diverse toxic gas molecules. It is fabricated with zinc ions, coordinated by four imidazolate rings.

Besides, non-metal-based photocatalysts have recently emerged for environmental detoxification. Kumar et al. (2019) explored carbon nitride, metal nitrides, phosphides, chalcogenides, perovskites and carbides nano-photocatalysts for environmental detoxification applications. They are expected to address issues posed by metal oxide-based semiconductors and are used as better alternative to metal oxides. Some of the metal oxide-based catalysts limitations include photo corrosion, self-oxidation, cost, limited spectral response, difficulty to recover the photocatalyst, thermal instability, recombination problems and ineffectiveness towards diverse kinds of pollutants.

Different parameters including the effect of photocatalyst crystallinity and crystal size, catalyst surface area, porosity (including pore structure and pore size), catalyst surface properties, adsorption capacity and catalyst support can influence the performance of photocatalytic oxidation processes (Mamaghani et al. 2017). According to the report presented by the authors, higher reaction rate is achieved when crystallinity of the catalyst used is higher, and with smaller crystal size. The structural features like surface area and porosity can greatly influence the photocatalytic activity. Without changing the surface chemistry, when the surface area is increased, there is more number of active sites available to enhance the photocatalytic activity. Apart from higher surface area of photocatalyst, the microporosity and interconnected pore system are another major reason for superior photocatalytic activity. The micropores retard the slip-away of pollutants from the photocatalytic coating by increasing its residence time on the porous structures, thereby increasing the likelihood of reactants adsorption and reaction on the surface. Heat treatment is considered to be a technique to alter the crystallinity and structural properties of a photocatalyst. Another important factor that changes the surface area available for catalytic activity is the catalyst surface density (i.e. catalyst loading) on the support material. As the number of coating layers of photocatalyst on the support material is increased, there is an increase in VOC conversion or higher removal rates consequently. The support material used will also affect the photocatalytic activity. The main purpose of immobilizing the photocatalyst onto a support material is to address the aggression and agglomeration-related negative outcomes. Hence, the support material must possess properties like high surface area, porosity and adsorptive affinity and must be stable under ultraviolet illumination.

Catalytic oxidation

The oxidation technique (converting organic compounds into harmless components: carbon dioxide and water) is divided into (i) catalytic oxidation, which is done using catalysts at normal temperatures: 205–595 °C and (ii) thermal oxidation, without the use of catalysts, oxidation at much higher temperatures. Though the latter one requires only heat and oxygen, its operational cost is very high considering the amount of activation energy needed to achieve high temperatures (operate at temperatures in excess of 815 °C) (Speight 2019). While in catalytic oxidation, the amount of energy needed to initiate the oxidation process is done only using a catalyst and hence the activation-energy barrier is lower. A major challenge that remains with this catalytic removal system is the art of selecting appropriate catalyst from the wide range of available catalysts. Perhaps there are three categories of catalysts that can be used for the oxidation of VOCs: (i) supported noble metal catalysts (ii) non-noble metal oxides (supported or unsupported) and (iii) mixed-metal catalysts. As per most of the studies reported, the oxide support is mainly to promote the activation of oxygen on the catalysts surface. For example, silica and zeolite-supported noble metal catalysts systems are widely used for formaldehyde catalytic oxidation, considering their high surface area and uniform/ordered pore size/structure (Chen D et al. 2020; Xu et al. 2018).

Kamal et al. (2016) presented a critical review including all these three categories of catalysts employed in catalytic oxidation process. They have focused on gold, palladium, platinum and mixed noble-metal based catalysts under the category of supported noble metal catalysts, which are considered to be the most promising due to their high efficiency for the removal of VOCs at low temperature even though they are quite expensive. The support material could be ceramic or metallic. Whereas, catalysts based on cobalt, nickel, titanium, manganese, copper, chromium, vanadium and cerium were discussed under the category of non-noble metal oxide-based catalysts, whose formaldehyde decomposition rate was observed to be high enough at ambient temperature and are considered to be promising low-cost alternative catalysts. This group of catalyst (using transition and rare earth metal oxides) could be supported (on clay, aluminosilicate and so on) or unsupported. For example, Arun and Gobi (2015) used magnesium aluminate ($MgAl_2O$) and magnesium titanate ($MgTiO_3$) nanoparticles (prepared by hydrothermal method) and embedded them into polyacrylonitrile nanofibrous membrane for the degradation of 2-chloroethyl ethyl sulphide (2-CEES), a stimulant of sulphur mustard. Here, electrospun nanofibrous membrane acted as the support material.

Also, there are some mixed-oxide catalysts (also termed as binary metal oxide) like Mn–Ce, Cu–Mn, Co–Ce, and Mn–Co that are widely researched for oxidation of different VOCs including formaldehyde, toluene, benzene, propanol, n-hexane, ethyl acetate (Kamal et al. 2016; Yi et al. 2018; Zheng et al. 2015; Wen et al. 2009). Research studies have shown that two-component transition metal oxide catalysts exhibit very high oxidation activity as compared to single-component metal oxides. That is, compared to individual

metal oxides, richer redox reactivity is witnessed with coupling of two metal species (Huang et al. 2016). Perhaps, with doping or addition of other metals there is a prominent change observed in the structure of metal oxides. There is generation of ion holes and oxygen vacancies, contributing to structural defects thereby increasing the redox ability with an increase in oxygen storage capacity and ultimately, enhancing oxidation activity of the catalysts. Huang et al. (2018a) used MnO_x–CeO_2 catalysts to investigate the oxidation of formaldehyde at ambient temperature. Though studies have shown that manganese oxide mesoporous materials exhibit impressive absorption capacity in formaldehyde oxidation with their interconnected network structures, their activity at ambient temperature was very poor. Hence, Huang and team designed and prepared catalysts by doping CeO_2 in MnO_x, which showed excellent low-temperature catalytic activity for formaldehyde oxidation. Wu et al. (2020) synthesized by co-precipitation method $MnCo_3MO_x$ (M = Ce, La, Pr) composite catalysts with the aim to achieve complete (100%) removal of formaldehyde at room temperature. Among the three rare earth metals (Ce, La, Pr) used to enhance the performance of $MnCo_3O_x$ catalyst ($MnCo_3Ce_3O_x$, $MnCo_3La_3O_x$, $M4nCo_3Pr_3O_x$), addition of Ce significantly improved reduction performance of $MnCo_3Ce_3O_x$. Its activity at a 1/3/7 M ratio of Mn/Co/Ce showed 100% removal of formaldehyde at room temperature.

The non-noble metal catalysts are a good alternative to the quite expensive noble-metal catalysts. Also the metal oxide-based catalysts are more tolerant to destruction process, compared to precious metal catalyst. The deactivation and regeneration of catalysts is one of the major problem associated with catalytic oxidation. The deactivation is done through different methods, including fouling, sintering or poisoning, thermal degradation, crushing, vapour compound formation and solid–solid reaction. This review will discuss the most recent works presented in the last 5 years with regard to catalytic oxidation (Table 1).

Evidently, there are three mechanisms proposed for catalytic oxidation of VOCs (Pei and Zhang 2011; Guieysse et al. 2008; Becker 2018). Depending on the type and characteristics of the catalyst and targeted VOC, either Langmuir–Hinshelwood, Eley–Rideal, or Mars-van Krevelen models will be used to explain the mechanism of catalytic degradation of VOC.

(i) Mars–van Krevelen model (redox or regenerative mechanism)

The literature concerning the oxidation of VOCs using this model considers a two-stage redox step to describe the total hydrocarbon oxidation on metal catalyst. The sequence of oxidation–reduction is assumed to occur on the metal oxide surface. As shown in equations below, first the adsorbed VOCs react with lattice oxygen on the solid catalyst surface thus reducing the metal oxide. In the second step, the reduced active site (or the reduced metal oxide catalyst) is re-oxidized by gas phase oxygen.

$$\text{OAS(Oxidized Active Site)} + A \rightarrow \text{AS} + \text{AO}$$

$$\text{AS} + {}^{1}\!/_{2}\, O_2 \rightarrow \text{OAS}$$

Where A is the Gas Phase Reactant, AO is the product of oxidation and AS is the reduced active site.

The general oxidation kinetic reaction is expressed as.

Rate of reaction, $R = \frac{RoRiCoCi}{(RoCo+\gamma RiCi)}$ where, Ro = oxygen chemisorption rate constant.

Ri = Surface reaction rate constant.

Co = oxygen concentration.

Ci = Hydrocarbon concentration.

γ = Stoichiometric coefficient for total oxidation or Stoichiometric coefficient of oxygen in the oxidation.

(ii) Langmuir- Hinshelwood model

As shown in Fig. 3a, this mechanism assumes that a bimolecular reaction takes place between two atoms that are adsorbed on the surface adsorption sites. It is, furthermore, assumed that once the reaction is complete, the as formed product will desorb from the surface.

Consider this bimolecular reaction as follows; where 'S' represents available surface active site for adsorption, 'X' and 'Y' represent the reactants.

$$X + S \rightleftharpoons \text{XS(adsorption of } X\text{)}$$

$$Y + S \rightleftharpoons \text{YS(adsorption of } Y\text{)}$$

$$\text{XS} + \text{YS} \rightleftharpoons P\,\text{(product)}$$

$$P \rightarrow P_g + 2S\text{(desorption of products)}$$

(iii)Eley–Rideal model

As shown in Fig. 3b, this mechanism assumes that a reactant molecule will be adsorbed on the surface site and will directly react with another incoming molecule form the gas phase, wshich implies that the incoming molecules would not require an adsorption site on the surface. Such reactions can be described as a non-thermal reaction.

$$X + S \rightleftharpoons \text{XS(adsorption of } X\text{)}$$

$$\text{XS} + Y \rightleftharpoons P\,\text{(product)}$$

$$P \rightarrow P_g + S\text{(desorption of products)}$$

Table 1 Oxidation techniques for formaldehyde decomposition

Oxidation Category	Catalyst	Temperature	Removal Performance	Activity Test Method	Reference
Photocatalytic	Nano-ZnO on bone char	Room temperature; Relative humidity ~ 35%	The maximum HCHO decomposition efficiency was 73%. The synergetic action on photocatalytic degradation of HCHO was mainly imparted because of the immobilization of ZnO nanoparticles onto the bone char	A system consisting of 3 sections: feed, photoreactor (made of Pyrex glass), and gas detection apparatus Light source: 8-W ultraviolet lamp emitting light at a wavelength of 365 nm Ultraviolet intensity: 1,180 microW/cm^2	Rezaee et al. (2014)
Non-noble mixed metal catalytic	$MnO_x - CeO_2$	100 °C	Mixed Mn/Ce oxides facilitated the complete oxidation of HCHO at lower temperature in comparison with pure CeO_2 and MnO_x oxides	The HCHO catalytic oxidation was performed in a fixed bed reactor, loaded with 200 mg of the catalyst. The catalyst was activated in situ at 250 °C for 2 h with 20% volume O_2 balanced by He, with a flow rate of 30 mL min^{-1}	Quiroz et al. (2015)
Catalytic	α-, β-, γ- and δ-MnO_2 catalysts (different crystal structures)	Low temperatures (~ 80 to ~ 150 °C)	δ-MnO2 exhibited nearly complete HCHO conversion at 80 °C, while the α-, β- and γ-type MnO2 obtained 100% only at 125 °C, 200 °C, 150 °C, respectively	Fixed-bed quartz flow reactor (i.d. = 4 mm) in an incubator; gas hourly space velocity (GHSV) of 100,000 mL (gcat h)$^{-1}$	Zhang et al. (2015)
Non-noble metal Catalytic	Layered MnO_x, (i.e. birnessite)	Room temperature	The activity of birnessite for HCHO oxidation was positively associated with its water content, i.e. the higher the water content, the better activity it had	The concentration of HCHO (initial concentration at ~200 ppm) in the glass bottle, with 50 mg of sample, was determined by using MBTH method	Wang et al. (2015a)
Catalytic	Graphene – MnO_2 Hybrid Nanostructure	65 ~ 100 °C	100% HCHO conversion at 65 °C and could be maintained up to 72 h Kinetic tests revealed that graphene has reduced the activation energy of MnO_2 catalyst from 65.5 to 39.5 kJ mol^{-1}	Fixed-bed reactor under atmospheric pressure Gas hourly space velocity (GHSV) of 30,000 mL (gcat h)$^{-1}$ 100 mg of catalyst	Lu et al. (2016)
Catalytic	$Co_xMn_{3-x}O_4$ nanosheets (binary metal oxide)	100 °C	100% of HCHO converted to CO_2 at a temperature of 100 °C. Also, exhibited very good catalytic stability	Fixed-bed reactor with catalyst (0.85 g); GHSV is 120,000 mL (gcat h)$^{-1}$	Huang et al. (2016)

Table 1 (continued)

Oxidation Category	Catalyst	Temperature	Removal Performance	Activity Test Method	Reference
Catalytic	Core–shell α-MnO_2@L-MnO_2 heterostructure α-MnO_2 nanotubes as the core and layered L-MnO_2 as the shell. Also, Trace Pt nanoparticles (1 wt%) were also coated over the MnO_2 samples	Room temperature	Compared to the Pt/α-MnO_2 and Pt/L-MnO_2, the Pt/ α-MnO_2 @L-MnO_2 displayed higher HCHO removal capacity 92.1% HCHO conversion over the Pt/α-MnO_2 @L- MnO_2, whereas 81.3% and 75.9% for the Pt/α-MnO_2 and Pt/L-MnO_2 (Upon 1 h treatment) respectively	6L organic glass box covered by a layer of aluminium foil on its inner wall. The concentrations of CO_2 and HCHO were recorded online using a Photoacoustic IR Multigas Monitor 100 mg catalyst powder	Zhou et al. (2017)
Photocatalytic	Bi_2O_3/TiO_2	Room Temperature	The HCHO concentration decreased from 1.031 to 0.061 mg/m^3 in 24 h. Experimental results clearly shows that, Bi_2O_3 doped TiO_2 samples exhibited better photocatalytic activity than TiO_2	In-house designed glass reactor connected to a PPM-400ST HCHO meter. 0.4 g portion of the photocatalyst powder was used. 36 W LED energy- saving lamp with a luminous flux of 2520 lm was used as the light source	Huang et al. (2018b)
Catalytic	Hollow MnO_2 spheres	~100 °C	Maintained a high 75% conversion up to 90 h of reaction, instead of the expected 50% conversion	Fixed-bed reactor (internal diameter = 10 mm) loaded with 200 mg catalyst With a gas hourly space velocity (GHSV) 30,000 h^{-1}	Boyjoo et al. (2018)
Photocatalytic	rGO/TiO_2 With the anatase TiO_2 nanoparticles dispersed uniformly on the surface of reduced graphene oxide	Room temperature (25 ± 1 °C)	88.3% of HCHO (the remaining concentration was 58.5 ppbV) was removed after 240 min of visible light irradiation Relative humidity was about 50% ± 5%	Self-made airtight stainless-steel cell with a quartz cover; xenon lamp (500 W) used as the light source; 0.2000 g photocatalyst	Yu et al. (2018)
Noble metal catalytic	Pt/ZSM-5 with nickel cation modification	30 °C	Removal efficiency of ~90% and a 100 h stable performance, achieved with a low 0.1-wt% Pt amount and ultralow 0.05-wt % Ni addition	Tests were carried out in a homemade fixed-bed reactor packed with 0.2 g catalyst. HCHO was introduced to the reactor with a gas hourly space velocity of 30,000 mL/hg and HCHO concentration was determined by phenol spectrophotometric method	Ding et al. (2018)
Plasma-promoted photocatalytic (under visible-light irradiation)	Au/TiO_2	Room Temperature	O_2 plasma activated catalyst presents an enhanced visible-light absorption and surface charge transfer efficiency in HCHO oxidation	A single-pass continuous flow reactor; HCHO simulated air (80% N_2 + 20% O_2) at a flow rate of 200 mL/min	Li et al. (2019a, b)

Table 1 (continued)

Oxidation Category	Catalyst	Temperature	Removal Performance	Activity Test Method	Reference
Catalytic	Pd/CeO_2	Room Temperature	The conversion of HCHO to CO_2 reached 89% and kept at over 80% during 300 min test Note: Non-thermal plasma was used to pre-treat and activate the catalyst. Thus sintering and agglomeration were avoided. Also, the Pd particle size was smaller with abundant surface-active oxygen species compared with thermally reduced catalyst	A continuous flow fixed bed quartz reactor. 40 mg of catalyst was placed between quartz wool layers in the reactor. Flow rate 100 mL/min and GHSV of 150,000 mL/g/h	Li et al. (2019a, b)
Photocatalytic	Bi_2MoO_6/Bi/g-C_3N_4 heterojunction. It was assembled with in-situ reductive Bi nanoparticles	Room Temperature	96.15% of HCHO (200 ppm) was oxidized to CO_2 and H_2O after six runs (total 60 h) and 98.80% for 1600 ppm under 10 h The impressive performance was attributed to Bi nanoparticle that is linking Bi_2MoO_6 and g- C_3N_4 together. It also contributes to good visible light harvesting. This material can also be used for the removal of other general gaseous pollutants (C_6H_6 and $CH_3COOCH_2CH_3$)	A closed photocatalytic reactor, under visible light irradiation (300 W xenon lamp, $\lambda > 420$ nm, 30 mW cm^{-2})	Wu et al. (2020)
Catalytic	CoMn oxides (Na or K doping mainly to improve its HCHO oxidation activity, especially at low temperatures (< 70 °C)	Room Temperature	Upon doping (especially with K) the generation of active surface oxygen species increased from 25% to ~ 40%. And HCHO rates increased from ~ 15 µmol/g/s to 25 µmol/g/s (with Na doping) and to ~ 60 µmol/g/s (with K doping) at 40 °C. Thus, CoMnK exhibits the highest activity for HCHO oxidation	Used fixed-bed quartz microreactor. 0.10 g sample (40–60 mesh) was sandwiched between quartz wool in the tube reactor. Paraformaldehyde was used to generate the gaseous HCHO; total flow rate was 100 mL/min; space velocity of 60,000 mL g^{-1} h^{-1}	Wang et al. (2020a, b)
Catalytic	Pt/TiO_2	50 °C and 100 °C	HCHO conversion efficiency reaches 98% and 100%	Catalytic oxidation reaction was operated in a fixed bed reactor under atmospheric pressure	Su et al. (2020)

Table 1 (continued)

Oxidation Category	Catalyst	Temperature	Removal Performance	Activity Test Method	Reference
Catalytic	MnO_2/AlOOH composite	Room Temperature	Higher ability to remove indoor low-concentration HCHO compared to the birnessite MnO_2 at room temperature	Static test method performed in a self-constructed reaction facility for HCHO removal	Liu Z et al. (2020)
Noble metal catalytic	Au@SiO_2 (Core–shell structures synthesized by soft-template method)	100 °C	100% HCHO conversion/removal	U-type quartz reactor (i.d. = 8.0 mm) under atmospheric pressure With a gas hourly space velocity = 15,000 mL/(gh)	Chen D et al. (2020)
Photocatalytic	β-Ga_2O_3 Nanostructures (Nanoparticles and nanorods)	Room temperature	The HCHO removal efficiency under deep ultraviolet irradiation (278 nm) of the synthesized β-Ga_2O_3 nanoparticles is higher than that of the β-Ga_2O_3 nanorods, with 82% and 62% HCHO removal efficiencies, respectively	Homemade system consisting of, HCHO precursors, reactor chamber, and monitoring chamber. 1.5 g of synthesized β-Ga2O3 nanostructures were used in the reactor Deep ultraviolet (UVC) lighting was used. UVC-LEDs (278 nm, 10 mW)	Lee et al. (2020)
Noble metal catalytic	3D manganese dioxide/carbon foam (MnO_2-CF) composite (Having a porous framework and a core–shell structure)	Room Temperature	Owing to large S_{BET}, abundant surface oxygen species, 3D hierarchical porous structure of Pt/MnO_2 -CF, it displayed the best HCHO oxidation activity (HCHO removal of 91% was achieved after 60 min) among others like CF, Pt/CF, MnO_2–CF, and Pt/MnO_2–MS (Pt/MnO_2 microsphere) at room temperature	Organic glass box reactor equipped with a photo- acoustic field gas monitor The HCHO adsorption activity was estimated noting the decrease of HCHO levels and the increase in concentration of CO_2 concentration	Ye et al. (2020)
Catalytic	Porous carbon spheres with well dispersed MnO_2 particles	Room Temperature	The HCHO removal efficiency remained 100% even after reaction for 20 h at room temperature over the ACS–O-6% Mn *ACS- activated carbon spheres	Evaluated at 25 °C in a fixed bed reactor; gas space velocity of 80,000 h^{-1}	Zhang et al. (2020a)
Photocatalytic	Cu-TiO_2 (By grafting nano CuO_x clusters onto TiO_2)	Ambient temperature	100% HCHO conversion to CO_2 within 140 min	Home-made flow reactor; 500 W commercial Xe lamp; light intensity at about 10.2 mW/cm^2; Relative humidity of 50%	Chen M et al. (2020)
Catalytic	Nb_2O_5 nanoparticles supported bimetallic nanocatalysts (IrxPt1-x/Nb_2O_5)	Moderate temperature	100% conversion at 30 °C	Fixed-bed quartz tubular reactor connected to online gas chromatograph; GHSV was varied from 60,000 to 240,000 ml $gcat^{-1}$ h^{-1} 0.2 g of catalyst sample	Ammar et al. (2020)

Table 1 (continued)

Oxidation Category	Catalyst	Temperature	Removal Performance	Activity Test Method	Reference
Photocatalytic	TiO_2 nanotube	Room Temperature	Highest absorption efficiency of 94.0%	HCHO degradation was performed in a sealed acrylic container (20 L) equipped with a rotating disc photo-catalytic fuel cell under UV irradiation Ultraviolet source: Two low-pressure mercury lamps (G8T5, 8 W, Philips)	Zhang et al. (2020b)

HCHO, Formaldehyde; MnO_x-CeO_2 Mixed metal oxides Cerium oxide; MnO_2, Manganese dioxide; GHSV- Gas hourly space velocity; ZnO, Zinc oxide; TiO_2, Titanium dioxide; CeO_2, Cerium oxide; MBTH—3-methyl-2-benzothiazolinone hydrazine; Co_xMn_3-xO_4 cobalt—manganese oxides; α-MnO_2@L-MnO_2—growth of layered Manganese dioxidenanosheets over α-MnO_2 nanotubes; Bi_2O_3/TiO_2—Titanium dioxide doped with Bismuth trioxide; *LED* Light-emitting diode; *ppbv*, parts per billion volume; rGO/TiO_2, Titanium dioxide nanoparticles immobilized on reduced graphene oxide; Pt/ZSM-5—Zeolite Socony Mobil-5 supported Platinum; C_6H_6—Benzene; $CH_3COOCH_2CH_3$—Ethyl acetate; Bi_2MoO_6—Bismuth molybdenum oxide; g-C_3N_4—Graphitic carbon nitride; AlOOH—aluminium oxyhydroxides; Ga_2O_3—Gallium oxide; MnO_2-CF, Manganese dioxide/carbon foam composite; ACS-O, Preoxidized activated carbon spheres; Nb_2O_5, Niobium oxide; Ir_xPt_{1-x}/Nb_2O_5, Niobium oxide Nanoparticles supported Platinum-iridium bimetallic nanocatalysts; G8T5, Germicidal Fluorescent Light Bulb

Adsorption

There is an increasing demand for simple, easy to operate and low cost, indoor formaldehyde removal methods, and this has stimulated research activities in the field of adsorption for formaldehyde removal. The adsorption process is generally classified as chemisorption (chemical adsorption, mainly through covalent bonding) and physisorption (Physical adsorption, mainly through weak van der waals forces). Micropore rich activated carbon, activated carbon fibre, silica, alumina, clay and zeolite with extremely high surface area (surface-to-volume ratio) are usually considered to treat VOCs like formaldehyde through physisorption (Suresh and Bandosz 2018). Activated carbon can be of different origin, for example it can be produced (by processes of carbonization and activation) from bamboo, wood, coal, rice husk, coconut shell, biomass, or it can even be produced from waste rubber tyres, plastic wastes, sugarcane bagasse and so on (Saleem et al 2019; Gopinath et al. 2020). Among the different types of adsorbents, carbon-based adsorbents such as graphene and its derivatives, carbon nanotubes, activated carbon, and biochar are the most common and widely used commercial adsorbent because of its attractive adsorbent properties like large specific surface area, pore size that fits the adsorbate size and the surface chemical functional groups. Another key parameter of carbonaceous adsorbent is the bulk density. The capture of VOCs per unit volume is more with higher carbon density and also, adsorbent regeneration need not be done frequently. However, unlike other indoor VOCs, formaldehyde has relatively higher vapour pressure (3890 mm Hg at 25 °C), lighter molecular weight (30 g/mol) and lower boiling point (− 19.3 °C), which in turn hinder the formaldehyde condensation in micropores of adsorbent. Hence, its removal from air only through physisorption (for example using only granular activated carbon) cannot be done very effectively.

Pei et al. (2011) illustrated three different pathways to express the interaction of water vapour and contaminants (formaldehyde in particular) in porous adsorbent media. (i) Competitive adsorption between water molecules and formaldehyde. As water vapour and formaldehyde have similar polarity and hence there is a competition for active sites at the exposed pore surface, reducing the formaldehyde adsorption capacity. (ii) Condensation of water vapour in the micropores. The amount of exposed surface area for adsorption of pollutant molecules reduces because of the capillary condensation of water in micropores. In this case, the presence of water reduces the adsorption capacity of an adsorbent by blocking its micropores. (iii) Apart from these two effects, water-solubility of the contaminant molecules in the already condensed or adsorbed water in pore sites of a sorbent is another effect. For example, the adsorbed

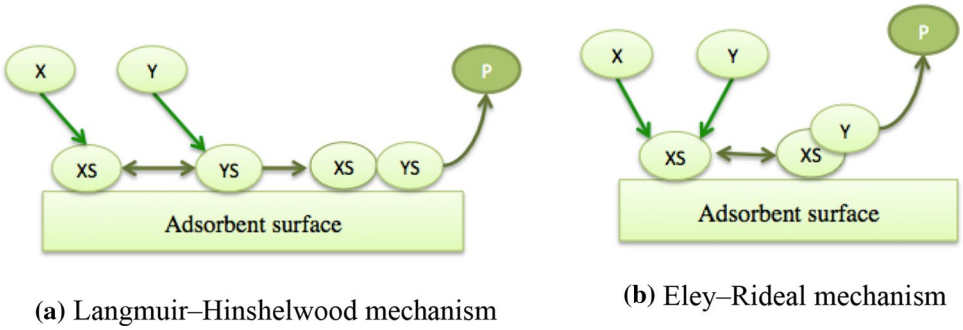

(a) Langmuir–Hinshelwood mechanism **(b)** Eley–Rideal mechanism

Fig. 3 Adsorption of gaseous species. **a** Langmuir–Hinshelwood, which explains reaction between adsorbates that are, adsorbed on the surface adsorption sites. 'S' represents available surface active site for adsorption, 'X' and 'Y' represents the reactants, 'XS' and 'YS' represents adsorption of reactants X and Y on S respectively, 'P' represents the product. **b** Eley–Rideal mechanism, where the adsorbed molecules react with impinging gas molecules directly through simple collision. This indicates there is a reaction between an adsorbate and an incoming molecule

water could contribute to an increased adsorption capacity, since formaldehyde is water-soluble. Perhaps, with an increase in relative humidity, the water content in the media increases, thereby letting hydrophilic formaldehyde dissolve in the adsorbed water. Here we can witness an increase in formaldehyde adsorption capacity. Whereas as seen earlier, the condensed water in micropores sometimes tend to block the available pores for adsorption. Hence the effect of relative humidity on chemisorption of formaldehyde is still controversial as its effect can be different for various materials.

Apart from relative humidity, temperature plays a significant role in formaldehyde or any VOC adsorption rate. Unlike some catalytic oxidation technique involving the use of high temperature for conversion of VOCs to non-toxic substance, adsorption is generally carried out at normal room temperature. However, with an increase or decrease in temperature below the optimal level has shown to affect the VOC adsorption rate. Therefore, it becomes important to find that optimal level of temperature, which varies with different sorbents. Kim et al. studied mesoporous MCM-41, zeolite, and amorphous silica, functionalized with three kinds of amine groups 3-aminopropyl- triethoxysilane (APTES), N(b-aminoethyl) g-aminopropylmethyl dimethoxysilane (AEAPMDMS), and N1-(3-(trimethoxysilyl)-propyl) diethylenetriamine (TMSPDETA) and investigated the effects of different temperature conditions (10–50 °C) on formaldehyde adsorption. At 30 °C, the adsorption efficiency was the highest, above which the adsorption efficiency decreased rapidly, suggesting 30 °C to be an optimum temperature level for interaction between amine and formaldehyde (Kim et al. 2011). Chiang et al. (2001) investigated the effects of pore structure and temperature on VOC adsorption on activated carbon. At high temperature, the benzene adsorption on bituminous coal and coconut shell-derived activated carbons increased notably (Chiang et al. 2001). Most of the studies showcase the fact that, at a higher temperature there is strong interaction between the adsorbent and adsorbate molecules, which increases the adsorption efficiency. Nevertheless, adsorption is n exothermic reaction. That is with an increase in temperature, entropy on the adsorbent surface increases, and the adsorbate gets desorbed with a decrease in adsorption bond strength. Therefore conclusively, with an increase in temperature there is a decrease in adsorption capacity (Jiun-Horng et al. 2008).

With the advent of nanotechnology, various nanomaterials can be potentially employed as a tool to interact with airborne pollutants with varying surface properties. Kebede et al. (2017) synthesized viscose rayon cellulose fibre (a flexible catalyst sheet) with Pt nanoparticles (dendrimer immobilized nanoparticles) loaded on them for removal of formaldehyde. This fibre-based catalytic system used poly (amido amine) dendrimer, an intermediator between Pt nanoparticles and the fibres. The dendrimer played a dual role of protecting (or stabilizing) the nanoparticles, help proper nanoparticles dispersion without aggregation and the terminal amine in dendrimer was used for formaldehyde adsorption. Yamanaka et al. (2013) prepared nanosized scallop shells (waste product from seafood industry) by dry ball milling process and then with subsequent addition of water. They have demonstrated that the ground shells (specific surface area ~ 54.4 m^2g^{-1}) have great potential to adsorb formaldehyde effectively. Wen et al. (2010) investigated adsorption and desorption performances of formaldehyde using high-performance and affordable activated carbon produced from sewage sludge and compared them with the commercially available activated carbons. Activated carbon produced from sewage sludge exhibited excellent adsorption performances when compared with commercial activated carbon, with initial removal efficiency of 83.72% and 89.56%, at formaldehyde concentration of 498 mg/m^3 and 0.41 mg/m^3, respectively.

Carbon nanotubes are also applied in many adsorption-based applications, due to their outstanding ability for the removal of various inorganic and organic pollutants since their discovery (Pan and Xing 2008; Ren et al. 2010; Shih and Li 2008). Compared to granular activated carbon, carbon nanotubes have been shown to be more effective in the removal of ozone. Yang et al. (2017) aimed to address the interactions between carbon nanotubes and formaldehyde. They developed a carbon nanotube/activated carbon fibre filter medium fabricated by in-situ growth of carbon nanotubes on activated carbon fibre, which exhibited superior formaldehyde adsorption capacity (almost three times more) than the normal activated carbon fibre filter medium (Yang et al. 2017). Moreover, activated carbon fibre by itself has superior properties. The micropore-rich fibre surface attributes to very high surface area (surface-to-volume ratio) between 2000 and 2500 m^2/g that encourages adsorption of wide range of organic pollutants (Gopinath et al. 2018).

Zhang et al. (2017) have summarized some of the common acidic and basic functional groups namely carboxyl, hydroxyl, carbonyl, anhydride, lactone, quinones, pyrone, chromene, pyrrole, pyridone and so on, along with their characteristics on carbonaceous adsorbents. The source or raw materials and modification treatments used to produce carbonaceous adsorbent may be responsible for the type of surface functional groups (oxygen-containing or nitrogen-containing) available on the adsorbent. Scientifically, their surface chemistry is mainly governed by the heteroatom (O, N, S, H, halogens etc.) of functional groups for enhanced surface and adsorption functionalities. Among them, the presence of oxygen functional groups (either Brönsted acidic or basic sites) and nitrogen containing groups are considered to be most important adsorption species.

The development of novel VOCs adsorption technology by modifying the surface chemistry of carbonaceous adsorbents is one key area of research. To control the properties and to modify surface functional groups of the final carbonaceous material, certain synthesis route involving post-treatment with chemical agents are considered. The nitrogen containing groups are introduced into the carbon framework, usually by heat treatment of carbon materials under NH_3 atmosphere, or introduced by ammonium, nitric acid, and N-containing compounds treatment, thus presenting a basic property and increasing the carbon surface polarity and π electrons (Li et al. 2018; Zhang et al. 2017). In general, nitrogenation is employed to introduce nitrogen-heteroatoms containing functional groups like $–NH_2$, –NH, –C=N and –C–N on carbon surface. Similarly, modification techniques like surface oxidation and sulphuration are used to introduce oxygen heteroatoms, containing functional groups like –OH, –COOH, –C=O, –C–O onto the surface of adsorbents and sulphur heteroatoms containing functional groups like C–S, C=S, or S=O onto the surface of carbon adsorbents respectively. Yang et al. (2019) in the year 2019 have clearly summarized these modification methods for introduction of heteroatoms for enhanced surface functionalities and sorptive properties for heavy metal adsorption (Yang X et al. 2019).

Such a modification, typically nitrogenation, with the amine functional group ($–NH_2$), is found to be the most adaptable approach to enhance formaldehyde adsorption efficiency. Researchers have well documented the amine-aldehyde chemical conjugation fact (formation of chemical bond between adsorbate and adsorbent) through covalent bonding to improve the formaldehyde adsorption capacity. As seen earlier, formaldehyde is adsorbed effectively on activated carbon or other adsorbents like alumina or silica only through physisorption. However, owing to stronger adsorption forces with other compounds as well, formaldehyde gets desorbed eventually to the air phase.

Therefore, an additional surface modification or enhancing the surface chemistry of adsorbent is of great interest with regard to VOC adsorption. Compared to unmodified activated carbon, graphite oxide and silica, it has been reported that the amount of formaldehyde adsorbed on the same materials containing amino groups (amine-functionalized materials) showed higher formaldehyde adsorption rates (Saeung and Boonamnuayvitaya 2008; Photong and Boonamnuayvitaya 2009; Ma et al. 2011). The reaction between amine and formaldehyde produces imine (compounds having – N=C= function; also known as Schiff bases, with its characteristics FTIR peak displayed around 1690–1640 cm^{-1} and its intensity increases with increased formaldehyde exposure time) with elimination of water in the reaction (Chen et al. 2016). The reaction process between carbonyl group of formaldehyde molecule reacting with the amino group on the surface of adsorbent material to form an imine group is shown in reaction below.

$$R - NH_2 + HCHO \rightarrow -NH^+ = CH_2$$

Furthermore, materials containing polymeric amines like poly(allylamine), polyethyleneimine and chitosan contains many nitrogen-containing functional groups, which plays an important role in increasing formaldehyde adsorption ability (Zhang et al. 2020c; Yang et al. 2011; Gesser and Fu 1990). Chitosan is a natural, renewable, biodegradable, environmental friendly and linear polysaccharide obtained by deacetylation of chitin (Shalbafan et al. 2020). Furthermore, many publications have reported that chitosan-supported adsorbents are effective in removing indoor formaldehyde. Nuasaen et al. (2013) developed chitosan and polyethyleneimine functionalized carboxylated hollow latex that can adsorb formaldehyde through nucleophilic addition of amines to carbonyls of formaldehyde, followed by the elimination of water molecules. Hollow latex-polyethyleneimine

possessed higher formaldehyde adsorption efficiency compared to hollow latex-chitosan. Yang et al. (2019a, b) prepared a promising biodegradable adsorbent for removal of indoor formaldehyde, by cross-linking β-cyclodextrin and chitosan in acidic aqueous solution with glutaraldehyde as the cross-linker. With the inlet formaldehyde concentration of 46.1 mg/m^3, formaldehyde adsorbing capacity was up to 15.5 mg/g at a temperature of 20 °C.

There is one thing that needs to be considered while using chitosan. Chitosan molecules are dissolved in acidic water, which leads to protonation of the amine groups in the acidic medium. Thus removal of acid remnants as a post-processing step is often required when using chitosan-based filter medium. This chitosan polycation (molecule or chemical complex having multiple cationic sites) can be neutralized using strong bases like sodium hydroxide, potassium hydroxide or sodium bicarbonate followed by washing copiously to render or regenerate the NH_2 groups of the chitosan (Llanos et al. 2015).

Another important point that must be taken into account every time we try to fix the modifier molecule on surface of adsorbent material is; "The Fixation method". To an adsorbent, the modifier (e.g. any amino-containing modifiers) can be fixed either through grafting or impregnation. Since the modifier molecules are fixed on the surface of adsorbent material mainly through physisorption (involving no chemical bonds), this method tends to be highly unstable. In such cases, especially the amino-containing modifiers may cause secondary pollution at higher temperatures. This is because the amino-containing modifiers are highly volatile. This is why grafting technique is considered to be more stable and an effective approach, mainly because there is a strong bond between the modifier and the adsorbent surface. Table 2 will summarize the studies on some major adsorbents and their performance over the last 10 years.

There are some major conclusions that could be drawn from the study when it comes to adsorption of formaldehyde on adsorbents. (1) Though the relative humidity does not significantly affect physical adsorption capacity of VOCs in general, adsorption capacity of an adsorbent is reduced by the presence of water vapour through pore blockage or competition between water and formaldehyde which are of same polarity. (2) Further, with an increase in temperature above certain optimum level, rapid desorption of the adsorbed contaminants is envisaged. If temperature is too low, then it affects VOC adsorption capacity because of the lack of energy available for efficient adsorption to take place. (3) Other than these environmental factors like temperature and relative humidity, the properties of adsorbent materials such as surface area, pore structure, availability of suitable functional groups play a vital role in increasing VOC adsorption performance. In particular, modifying the surface properties of adsorbents with S- and N-containing functional groups (typically amines) significantly influence the adsorption capacity.

Nanofibrous membrane in formaldehyde filtration

With the advent of nanoscience and nanotechnology, air filtration and purification of polluted gas (both outdoor and indoor) have taken new avenues. As seen in earlier two sections, nanoparticles have played a major role both as a catalyst and as an adsorbent in formaldehyde removal. Similarly, the novel nanofibrous membranes because of their high versatility have attracted much attention from researchers and have been introduced for various applications, including biomedical applications, oil–water separation, water-purification, for sensors, waterproof and breathable clothing and so on (Gobi et al. 2018; Senthil et al. 2018; Li et al. 2019a, b; Wang et al. 2015b; Madhura et al. 2018). Due to their tremendous ability like large surface area, higher porosity with small pore size, high gas permeability, good surface adhesion, and light weight nature, development of electrospun nanofibrous membrane-based air filters are very active among researchers since the late 1980s (Berly and Nallathambi 2020). One benefit of using electrospun nanofibrous membrane is that the nanoparticles can be easily added into the polymeric solution to get the desired functional properties on the composite fibres. But the loading of nanoparticles must be done properly, because with higher nanoparticle loading there is agglomeration of nanoparticles that would in turn reduce the adsorption capacity.

Up until now, activated carbon and activated carbon fibres are the most commonly used material for VOC adsorption. However, compared to these materials, porous carbon nanofibres have become an area of intense interest for energy storage, catalysis and filtration applications due to their superior properties, like abundant available micropores, large surface area, and excellent adsorption capacity (Lee et al. 2010; Song et al. 2007; Wang et al. 2013; Kong et al. 2013; Katepalli et al. 2011). Lee et al. (2010) prepared electrospun polyacrylonitrile-based nanofibres, which were later carbonized and steam-activated to produce polyacrylonitrile-based activated carbon nanofibres with shallow and homogeneous microporous structure, for highly efficient formaldehyde adsorption. Formaldehyde adsorption ability was greatly increased because the carbon nanofibres possessed abundant nitrogen-containing functional groups. Thus, even at a low formaldehyde concentration, remarkable amount of formaldehyde was adsorbed onto the pore surface of the polyacrylonitrile-based activated carbon fibres, which was very high as compared to conventional activated carbon fibres. The nitrogen contents on carbon nanofibres played a dominant role in formaldehyde adsorption. Rong et al.

Table 2 Chemisorbents and their performance for formaldehyde removal

Adsorbent	Test Method	Performance	Reference
MCM-41, zeolite, and amorphous silica, functionalized with three kinds of amine groups APTES, AEAPMDMS, TMSPDETA	The adsorbent put into 5 L aluminium bag; concentration of HCHO was at 1.0 ppm; HCHO gas detection tubes were used to measure the adsorption capacity Temperature: 20 °C	TMSPDETA amine functionalized mesoporous material (MCM-41) showed the best adsorption performance. Whereas AEAPMDMS was the best amine group for microporous zeolite	Kim et al. (2011)
Activated carbon was modified by HMDA 3 different loading amount of HMDA: 0.01, 0.04 and 0.1 g HMDA/g activated carbon	Continuous flow fixed-bed reactor; 2.2 ppm of HCHO; 1.15gm of activated carbon; Flow rate: 1.5 dm^3/min Temperature: 298 K and 30% Relative humidity	The amount of HCHO adsorbed activated carbon with 0.04 HMDA loading was calculated to 3.80 mg/g. Too much HMDA resulted in decrease of HCHO adsorption	Ma et al. (2011)
Bone char modified with acetic acid	Reactor in a continuous flow mode; 100 mg adsorbent; HCHO concentrations 20, 50, 100 and 200 mg/L Temperature: 25 °C	The adsorption of HCHO was significantly increased with the presence of hydroxyl and carboxyl groups on the bone char surface	Rezaee et al. (2013)
Bamboo based activated carbon was modified by attaching silver (Ag) and copper (Cu) nanoparticles	Equipment with a research grade air flowed and passed through HCHO solution in a HCHO vapour generator to produce HCHO gas. The HCHO concentrations were measured using GC/FID The HCHO removal using activated carbon-Ag or activated carbon-Cu was evaluated at room temperature	Activated carbon-Cu was able to adsorb 0.341 mg/g HCHO compared to 0.264 mg/g with activated carbon alone. However, The concentration of HCHO removed by the activated carbon-Ag was highest (around 0.425 mg/g)	Rengga et al. (2013)
Amine-functionalized mesoporous silica (SBA-15) SBA-15 was functionalized by three aminosilanes, thus creating 3 aminosilica adsorbents (with primary, secondary, and tertiary amines)	The silica (15 mg) was enclosed in a gas sampling bag to which10 µL of aqueous solution of HCHO (10 wt%) was injected; 100 ppm initial HCHO concentration; HCHO concentration was determined using US EPA method TO-11/IP-6A	The most effective HCHO adsorbent (1.4 mmol g^{-1}) was found to be the aminosilica containing primary amines, and aminosilica containing secondary amines that showed quite low adsorption capacity (0.80mmolg^{-1}). Aminosilica containing tertinary amines showed very negligible HCHO adsorption capacity	Nomura and Jones (2013)
Hierarchical hollow silica microtubes (HHSM) Sol–gel method was used, TEOS was used as precursor and CTAB and bio-template polar catkin was used as co-templates	0.1 g of adsorbent was dispersed on the bottom of an organic glass box covered by a layer of aluminium foil paper on its inner wall At ambient temperature	The maximum HCHO adsorption capacity was noted to be 20.65 mg/g This is much higher when compared to the recent works using APTMS modified diatomite (8.95 mg/g) (Liu et al. 2019) and Graphene-like boron nitride (19 mg/g) (Ye et al. 2016)	Le et al. (2013)
Amino functionalized (using ethylenediamine) graphene sponge (G/S) and graphene sponge decorated with graphene nanodots (G-GND/S)	Two mainly used parts: (i) HCHO gas generator (ii) Adsorption and detector equipment The average weight of G-GND/S used was ~ 70 mg	The maximum HCHO adsorption capacity was noted to be 22.8 mg/g, which was displayed by G-GND/S. The better adsorption property is attributed to the high concentration of amine groups on G-GND/S surface in comparison to G/S (HCHO adsorption capacity was noted to be around ~ 7.5 mg/g)	Wu et al. (2015)
Hierarchical titanate nanospheres with amine grafters (using diethylenetriamine (DETA))	Test was performed in a manmade organic glass box reactor covered with aluminium foil on its inner wall, at room temperature; 0.1 g of sample; 200 ppm HCHO	DETA introduced into the synthesis system has shown to improving the HCHO adsorption performance. However, excessive mole ratio of DETA to titanium (IV) butoxide during the synthesis process is found to contribute quite less to the improvement of adsorption capacity. Also, affects the structure of synthesized titanate products	Chen et al. (2016)

Table 2 (continued)

Adsorbent	Test Method	Performance	Reference
Highly porous boron nitride having network of hexagonal boron nitride nanosheets	Test was performed in an organic glass box reactor and at 25 °C in dark	The Graphene-like boron nitride has high specific surface area (627 m^2/g) with abundant surface hydroxyl and amine groups. The maximum HCHO adsorption capacity was noted to be 19.0 mg/g, with ~ 20 ppm HCHO in air	Ye et al. (2016)
Carbon nanotubes-enhanced amino-functional graphene aerogels (GN/E) To support and connect the graphene layers carbon nanotubes were used. It also diminishes the aggregation effect and decreases the pore diameter Ethylenediamine was used to get the amino-functional G/E	Three mainly used parts: (i) HCHO generator (ii) Adsorbent (iii) detector equipment Gaseous HCHO was prepared through a dynamic volumetric method 100 mg adsorbent sample was imported into the system	Carbon nanotubes-enhanced amino-functional graphene aerogels exhibited an adsorption capacity of 27.4 mg/g for HCHO. The use of carbon nanotubes exposed more amino functionalities for the HCHO removal; also the well-defined smaller pore size enhanced the physical capturing of HCHO molecules	Wu et al. (2017)
Activated carbon fibres with surface modified by diethylene triamine (DETA)	Dynamic adsorption experiment using glass tubular reactor and outgassed at 373 K in a He flow; HCHO concentration = 50 ppmv Temperature: 298 ± 1 K with a gas flow rate of 300 $cm^3 \cdot min^{-1}$	~ 100-fold increase of adsorption capacity with DETA loading as compared to activated carbon fibres alone	Baur et al. (2018)
Amine-modified diatomite (Grafting was done using 3-aminopropyltrimethoxysilane)	-	Maximum HCHO adsorption capacity of 8.95 mg/g at 25 °C was noted with aminopropyltrimethoxysilane -modified diatomite, which is larger than that of commercially available activated carbon (1.01 mg/g) Whereas, HCHO adsorption capacity of unmodified diatomite was only 0.038 mg/g	Zhu et al. (2019)
Biodegradable Chitosan Grafted β–Cyclodextrin (β-cyclodextrin) via glutaraldehyde The introduction of β- cyclodextrin form inclusion complexes with organic and inorganic molecules. The adsorption capacity was improved with a combination of hydrophilic exterior created by the β-cyclodextrin and the hydrophobic cavity. Grafting β-cyclodextrin onto the chitosan also improved the stability and recoverability of adsorbents	The adsorption test was carried out in a shell-tube structured quartz fixed-bed reactor. 0.5 g of adsorbent was packed in the tube inside. The inlet HCHO concentration was 46.1 mg/m^3 with GHSV of 28 mL/min, and temperature of 20 °C The phenol spectrophotometric method was used to analyze the HCHO concentration in the inlet and the outlet gas stream	The HCHO adsorbing capacity was up to 15.5 mg/g. It has been shown through the experimental results that the adsorption performance was greatly improved with the presence of abundant amino and hydroxyl groups in the modified chitosan	Yang et al. (2019a, b)
Polyethyleneimine modified activated carbon The activated carbon modification with polyethyleneimine contributes to an enhanced HCHO adsorption efficiency because of the presence many hydrophilic groups, such as amino groups, hydroxyl groups, and carboxyl groups. Also, there are many nitrogen, and oxygen-containing functional groups	Column adsorption studies, with the experimental apparatus consisting of two main sections, (i) preparation of gas-VOCs vapour mixture, (ii) adsorption process in the fixed bed The glass column was packed with the 50 g of adsorbent. The initial HCHO concentration was controlled at 50 mg/L, and the flow rate of the gas mixture was maintained at 200 mL/min	The HCHO adsorption capacity is 190.1 mg/g by unmodified activated carbon, which is about 1.67 times less than polyethyleneimine modified activated carbon (317.6 mg/g) with only 10 g/L of polyethyleneimine addition to activated carbon	Zhang et al. (2020a, b, c)

Table 2 (continued)

Adsorbent	Test Method	Performance	Reference
Polyaniline /TiO2 composite Polyaniline is identified to exhibit intrinsic redox properties; can exist in the different oxidation forms, and has fascinating doping and de-doping capabilities	Test was performed in an organic glass cavity (volume of 100 L) at ambient temperature, with 0.5 g of adsorbent dispersed at the bottom of glass Petri dish. The initial concentration of HCHO was controlled around ca. 0.5 ppm	The composite demonstrated increased adsorption capacity of 0.67 mg/g, which was higher capacity when compared to the commercially used activated carbon (0.50 mg/g)	Zhu et al. (2020)
Covalent organic polymers (porous polymeric materials consisting of 2D or 3D architecture involving covalent bonds) Functionalized with ethylenediamine and diethylenetriamine	Gaseous primary standard (G-PS) cylinder containing a mixture of 5 aldehydes was used. By injecting 20 micro L of formalin solution into a polyester aluminium bag filled with N2 gas, to prepare the HCHO G-PS. The adsorbent bed used 5 mg of the given adsorbent into a quartz tube	The adsorptive removal of a six-component aliphatic aldehyde gas phase mixture including HCHO was investigated. The HCHO adsorption capacity was found to be 14 mg/g	Vikrant et al. (2020b)
Activated carbon incorporated with (i) nitrogen and sulphur heteroatoms via a solvothermal process (AC-1) (ii) nitrogen and sulphur heteroatoms via a MW-based process (AC-2) (iii) nitrogen and silicon heteroatoms via a solvothermal process (AC-3) Commercial microporous activated carbon (AC-0) was used for modification	Packed-bed column filled with 5 mg of the prepared sample. Monitoring was carried out by the standard ASTM D5197 method	The HCHO adsorption capability followed the order AC-3 (1.17 mg/g) > AC-2 (1.04 mg/g) > AC-1 (0.13 mg/g) > AC-0 (0.11 mg/g) HCHO molecules reacted with the amine and sulfonic functionalities present on modified activated carbon through Mannich coupling (Schiff base mechanism) and α- hydroxymethanesulfonate formation reactions, respectively	Vikrant et al. (2020a)

HCHO, Formaldehyde; APTES—3-aminopropyl- triethoxysilane; AEAPMDMS g-aminopropylmethyl dimethoxysilane; TMSPDETA—N1-(3-(trimethoxysilyl)-propyl) diethylenetriamine; MCM-41—Mesoporous Silica—Mobil Composition of Matter No. 4; HMDA—Hexamethylene diamine; GC/FID—gas chromatography–flame ionization detection; SBA-15 Silica mesoporous—Santa Barbara Amorphous-15; ppmv, parts per million by volume; US EPA, United States Environmental Protection Agency; G-GND/S, Graphene sponge decorated with graphene nanodots; DETA, diethylenetriamine

(2003) studied the influence of heat treatment and its effect on formaldehyde adsorption over rayon-based activated carbon fibre. The heat treatment had significantly increased the formaldehyde adsorption capacities (roughly 24 mg/g). The adsorption capacity was much higher when compared to most of the recently undertaken works (Kadam et al. 2018, 2020) of formaldehyde adsorption.

Besides activated carbon nanofibres, there are other polymers like polystyrene, polyurethane, chitosan and so on (Scholten et al. 2011; Ge et al. 2016; Chu et al. 2015; Sargazi et al. 2019), that can be used to produce electrospun nanofibrous membranes, showcasing promising sorption capacities for VOCs. These membranes can be easily regenerated by desorption through simple nitrogen purging process under ambient conditions. The VOC removal potential of a nanofibrous material is influenced by surface chemistry of the material. Hence, considering polymers that are rich in functional groups are promising candidates for VOC removal. Many researchers have considered the use of cyclodextrins (cyclic oligosaccharide) and cyclodextrin-functionalized materials for VOC adsorption applications by exploiting their ability to form non-covalent host–guest inclusion complexes with toxic pollutants (Kayaci et al. 2014; Uyar et al. 2010; Celebioglu and Uyar 2018; Celebioglu et al. 2016). Soy protein (isolated component of soybean)-based nanofibrous membranes have been used for formaldehyde removal, mainly because of the presence of ionizable groups and many other functional groups, including polar, nonpolar, hydrophobic and hydrophilic ones (Nallathambi et al. 2019). Various other nanofibrous membranes especially surface modification with organic amines have been developed for scavenging indoor formaldehyde pollutant and is discussed in Table 3. It should be noted that the main advantage of employing easy to handle nanofibrous membrane-like morphology is an easy and effective way to stop leaching out of catalyst nanoparticles or adsorbents from the filter medium. Table 3 will showcase few research works based on nanofibrous membranes, with or without the presence of certain additives for formaldehyde removal.

Conclusion

Various technologies are introduced to address and remove the indoor air pollutants, considering the adverse effects of VOCs on human health. In this paper, we explored the diverse techniques currently used, with an emphasis on catalytic oxidation, adsorption and the use of nanofibrous membrane for removal of pollutants (especially indoor formaldehyde) from air. Among these technologies, adsorption has a high potential to adsorb the VOCs from air to the solid phase. Its dominance rests primarily on its simplicity, ease of operation and low cost. Yet it has faced challenges like saturation, pore blockage and thus the need for frequent regeneration of adsorbents, which in turn increases cost associated with the system. Similarly, even with photocatalytic process, catalyst's short lifetime due to loss of photocatalyst active sites can impose frequent catalyst replacement. Moreover, they are known to be effective in higher VOC concentrations (it isn't much effective at lower pollutant concentration) and generate secondary pollutants as well. Although photocatalytic oxidation is an effective technique owing to its room temperature operation and in removing a wide range of air pollutants mainly by converting harmful formaldehyde into benign, odourless and environmentally friendly components like H_2O and CO_2, the commonly used ultraviolet light source is quite expensive. Hence more research should be focused to increase the removal capacity under visible light conditions. Catalytic oxidation on the other hand is considered to be the most promising solution and it has high efficiency in removal of VOCs at low temperatures. At the same time, it is also non-economical because it requires noble metals as catalysts. Their practical use (mainly in industries) is restricted because they have poor thermal stability at temperatures above 500 °C. Hence transition-metal oxides with good thermal stability, which are cheaper, display good catalytic performances and are available in plenty is mostly considered. Further, employing nanofibrous membrane-like morphology has certain advantage, as it stops the leaching out of catalyst nanoparticles or adsorbents from the filter medium and increases the density of available active sites for pollutant interactions. These nanofibrous membranes can be costly and their operation/maintenance is expensive. Despite these obstacles, there are advantages associated with every technique. It is the role of researchers to identify the right technique for the target component and move towards hybrid systems, for example photocatalysts can be doped with adsorbent species or adsorbents can be immobilized on nanofibrous membrane or nanofibrous membranes can be functionalized with favourable functional groups (amines for example) for VOC abatement. Conclusively, to solve problems associated with every technique and for the development of these age-old techniques with effective and low-cost materials that can operate at normal room temperatures requires more research.

Author contributions BR: Conceptualization, Methodology, Investigation, Writing Original draft preparation. GN: Supervision, Review and Editing.

Funding The authors gratefully acknowledge the support from the Council of Scientific & Industrial Research (CSIR), New Delhi, India, to carry out this review work successfully. (Sanction number – 09/468/(0535) 2019 EMR – I).

Data availability Yes**,** demonstrating absolute data transparency.

Table 3 Nanofibrous membranes for formaldehyde removal

Polymer and solvent used	Additives and their properties	Note with observation	Reference
Polyacrylonitrile polyacrylonitrile -based activated carbon nanofibres	–	In dry and humid conditions the HCHO adsorption of polyacrylonitrile -based carbon nanofibres were very impressive as compared to conventional activated carbon fibres. Even at a low HCHO concentration (~11 ppm), remarkable amount of HCHO was adsorbed onto pore surface of the nanofibres	Lee et al. (2010)
Gelatin (18 wt%) Mixed solvent volume ratio (acetic acid: DI water = 80:20)	–	Gelatins are natural protein biopolymer rich in functional groups like amines (provided by amino acids such as lysine) and can lead to a powerful nanofibrous material for trapping toxic gases including HCHO. In this study instead of using toxic solvents, non-toxic solvent system was employed By increasing areal density of the filter from 2.25 to 3.80 g/m^2, HCHO capture capacity increased from 65.0% to 83.0%	Souzandeh et al. (2013)
Polyacrylonitrile, DMF as solvent	MOF ZIF-67 Mainly used because of their large surface areas, adjustable pore sizes and other controllable properties	The ZIF-67@polyacrylonitrile nanofibrous flexible filters were able to achieve 84% HCHO removal efficiency. Furthermore, BET surface area of ZIF-67@polyacrylonitrile filter is 532.6 m^2/g, whereas its only 15.7 m^2/g for pure polyacrylonitrile filter. This comparatively increased surface area and enhanced gas adsorption capability is attributed to abundant porous structure of the ZIF-67 nanocrystals	Bian et al. (2018)
Poly (vinyl pyrrolidone)	Supported Pt/electrospun TiO_2 nanofibre catalysts with a hierarchical macro-/meso-porous structure	The membrane was used for oxidative decomposition of high-concentration HCHO (140 ppm) at room temperature. The Pt/TiO_2 nanofibre catalyst system maintained a stable and efficient catalytic performance upto 4 cycles	Nie et al. (2014)
Sepiolite (or fibrous natural clay mineral), a hydrated magnesium silicate ($Si_{12}Mg_8O_{30}(OH)_4(OH_2)_4 \cdot 8H_2O$)	Noble metal platinum nanoparticles The highly dispersed nanoparticles on nanofibres are mainly for usual catalytic oxidation of HCHO and increasing the specific surface area	There existed abundant hydroxyls on the catalyst surface, which is most important for the catalytic oxidation of HCHO The excellent HCHO removal performance of Pt/sepiolite catalyst was ascribed mainly to the hydroxyls on sepiolite nanofibres and the Pt nanoparticles. At ambient temperature, 1wt% of Pt catalyst exhibited highest catalytic activity and the same performance lasted for 7 more cycles	Ma and Zhang (2016)

Table 3 (continued)

Polymer and solvent used	Additives and their properties	Note with observation	Reference
Polyacrylonitrile (9wt%), DMSO as solvent	β-cyclodextrin Due to its external hydrophilic groups (hydroxyl) and its hydrophobic inner cavity, it can form host–guest complexes with organic molecules The polyacrylonitrile fibres were both physically or chemically functionalized with β- cyclodextrin	β-cyclodextrin was added to polyacrylonitrile through two methods. First method involved addition of β-cyclodextrin to polyacrylonitrile solution before electrospinning it and secondly β- cyclodextrin was crosslinked on electrospun polyacrylonitrile fibres by alkaline hydrolysis and esterification with citric acid. The former one showed more HCHO capture efficiency than fibres obtained by crosslinking of β-cyclodextrin. According to the researchers, this may have happened because during the esterification process, the free hydroxyl groups on the β-cyclodextrin molecule would have been modified	Caro and Lainez (2016)
Poly (vinyl alcohol) (8.5 wt%) Mixed solvent (acetic acid/deionized water = 80:20, v/v)	Soy protein isolate Presence of ionizable and many other functional groups, including polar, nonpolar, hydrophobic, and hydrophilic ones	The HCHO removal efficiency was found to be 62.50%. In particular, the neat poly (vinyl alcohol) nanofabric showed a much lower HCHO removal efficiency of only 31.23%, indicating major role of soy protein isolate in removing HCHO	Souzandeh et al. (2016)
Polyacrylonitrile (9wt%), DMSO as solvent	β-cyclodextrin The cavity of β-cyclodextrin can be a host for HCHO molecules	polyacrylonitrile/β-cyclodextrin electrospun nanofibrous membrane, good HCHO adsorption (0.07 mg/g)	Kadam et al. (2018)
Poly (vinyl alcohol) (10 wt%) Water as solvent	Zeolitic imidazolate framework-8 (ZIF-8)@SiO_2 Silica based membranes possess active hydroxide groups and unsaturated residual bonds making them favourable for different modifications ZIF-8, a novel porous crystalline MOF with its pore space for HCHO or any gas storage	Formaldehyde adsorption capacities and physical properties of ZIF-8@SiO_2 membranes were compared to other materials like zeolite, activated carbon, aminosilica and few others. With ZIF-8@SiO_2 composite membrane (surface area SBET of 571 m_2/g) exhibited 48.87 mg/g of HCHO adsorption capacity	Zhu et al. (2019)
PMMA@PDA	Platinum–nickel nanoparticles (PtNi nanoparticles)	The membrane exhibited 90% HCHO (10 ppm) conversion at room temperature, only using a dosage of 0.02 g. It also retained its high activity for 100 h showing good flexibility and long-term stability. This superior catalytic performance is attributed to formate oxidation and mainly because of the presence of plenty of Pt–OH–Ni interfaces in nanoparticles used	He et al. (2019)
Polyvinylpyrrolidone (5wt%) Ethanol as solvent	Birnessite type manganese dioxide nanoparticles modified silica-doped titanium dioxide (MnO_2@SiO_2–TiO_2)	MnO_2@SiO_2–TiO_2 nanofibrous membranes exhibited high HCHO removal efficiency (100%) within 20 min. HCHO removal efficiency was mainly influenced by the MnO_2 nanoparticles-loading amount. The as-prepared catalytic materials showed 91.57% catalytic performance even after 5 cycles	Cui et al. (2019)

Table 3 (continued)

Polymer and solvent used	Additives and their properties	Note with observation	Reference
Polystyrene porous nanofibres THF as solvent	Birnessite-type MnO_2 Considering its low cost when compared to noble metals, and due to its high mobility of oxygen species, thermal stability, and ability to exhibit several tunnel structures	MnO_2/Polystyrene hierarchical porous nanofibre membrane exhibited high HCHO removal efficiency of 88.2% during its initial run and 74% was observed after five cycles	Hu et al. (2020)
Polystyrene (8 ~ 16 wt%) DMF as solvent	ZIF-67@ Polystyrene/$Co(AC)_2$ Cobalt acetate was added to polystyrene to produce cobalt acetate/polystyrene nanofibrous membrane and ZIF-67 MOF was grown on them	ZIF-67@Polystyrene nanofibre membrane showed maximum HCHO adsorption capacity than pure polystyrene nanofibre membrane. The HCHO concentration dropped to 0.55 mg/m^3 in just 4 min from its initial 2 mg/m^3 concentration and to 0.17 mg/m^3 in 8 min	Liu F et al. (2020)
Gelatin (16 wt%) Formic acid as solvent	β-Cyclodextrin	Gelatin/β–cyclodextrin composite nanofibre mats showed excellent adsorption of HCHO (0.75 mg/g) as compared to their previous work (Kadam et al. 2018) where the HCHO adsorption was only 0.07 mg/g. However, gelatin/β-cyclodextrin still couldn't reach the removal efficiency achieved using activate carbon fibres (Rong et al. 2003)	Kadam et al. (2020)

HCHO, Formaldehyde; *BET* Brunauer–Emmett–Teller; DMF, Dimethylformamide; DMSO, Dimethyl sulfoxide; SiO_2, Silicon dioxide; $Si_{12}Mg_8O_{30}(OH)_4(OH_2)_4.8H_2O$, Sepiolite a hydrated magnesium silicate; PMMA@PDA, polydopamine-coated polymethyl methacrylate electrospun fibre; THF, Tetrahydrofuran; $Co(AC)_2$, obalt acetate; ZIF-67, Zeolitic imidazolate framework-67; *MOF* Metal–organic frameworks

Code availability Not applicable.

Compliance with ethical standards

Conflict of interest The author declares that they have no conflict of interest.

Ethical approval Not applicable.

Consent to participate All authors agree with the content and that all have given consent to submit.

Consent for publication All authors agree for the publication.

References

Aguado S, Polo AC, Bernal MP, Coronas J, Santamaria J (2004) Removal of pollutants from indoor air using zeolite membranes. J Membr Sci 240(1–2):159–166. https://doi.org/10.1016/j.memsci.2004.05.004

Ammar SH, Salman MD, Shafi RF (2020) Catalytic activity of niobium oxide supported bimetallic nanocatalysts (Ir_xPt_{1-x}/Nb_2O_5) for oxidation of formaldehyde at moderate temperature. Colloids Interface Sci Commun 38:100305. https://doi.org/10.1016/j.colcom.2020.100305

An JY, Kim S, Kim HJ, Seo J (2010) Emission behavior of formaldehyde and TVOC from engineered flooring in under heating and air circulation systems. Build Environ 45(8):1826–1833. https://doi.org/10.1016/j.buildenv.2010.02.012

Baker RW, Yoshioka N, Mohr JM, Khan AJ (1987) Separation of organic vapors from air. J Membr Sci 31(2–3):259–271. https://doi.org/10.1016/S0376-7388(00)82232-2

Basavarajappa PS, Patil SB, Ganganagappa N, Reddy KR, Raghu AV, Reddy V (2020) Recent progress in metal-doped TiO_2, non-metal doped/codoped TiO_2 and TiO_2 nanostructured hybrids for enhanced photocatalysis. Int J Hydrog Energy 45(13):7764–7778. https://doi.org/10.1016/j.ijhydene.2019.07.241

Baur GB, Spring J, Minsker LK (2018) Amine functionalized activated carbon fibers as effective structured adsorbents for formaldehyde removal. Adsorption 24:725–732. https://doi.org/10.1007/s10450-018-9974-x

Becker C (2018) From Langmuir to Ertl: the "nobel" history of the surface science approach to heterogeneous catalysis. Encycl Interfacial Chem 99–106. https://doi.org/10.1016/B978-0-12-409547-2.13527-9

Berly R, Nallathambi G (2020) A concise review on electrospun nanofibres/nanonets for filtration of gaseous and solid constituents (PM2.5) from polluted air. Colloids Interface Sci Commun 37:100275. https://doi.org/10.1016/j.colcom.2020.100275

Bian Y, Wang R, Wang S, Yao C, Ren W, Chen C, Zhang L (2018) Metal–organic framework-based nanofiber filters for effective indoor air quality control. J Mater Chem A 6(32):15807–15814. https://doi.org/10.1039/C8TA04539A

Boyjoo Y, Rochard G, Giraudon JM, Liu J, Lamonier JF (2018) Mesoporous MnO_2 hollow spheres for enhanced catalytic oxidation of formaldehyde. Sustain Mater Technol 20:e0091. https://doi.org/10.1016/j.susmat.2018.e00091

Caro DN, Láinez MA (2016) Functionalization of polyacrylonitrile nanofibers with β-cyclodextrin for the capture of formaldehyde. Mater Des 95:632–640. https://doi.org/10.1016/j.matdes.2016.01.106

Celebioglu A, Sen HS, Durgun E, Uyar T (2016) Molecular entrapment of volatile organic compounds (VOCs) by electrospun cyclodextrin nanofibers. Chemosphere 144:736–744. https://doi.org/10.1016/j.chemosphere.2015.09.029

Celebioglu A, Uyar T (2018) Cyclodextrin short-nanofibers using sacrificial electrospun polymeric matrix for VOC removal. J Incl Phenom Macrocycl Chem 90:135–141. https://doi.org/10.1007/s10847-017-0764-y

Chen D, Shi J, Shen H (2020a) High-dispersed catalysts of core–shell structured $Au@SiO_2$ for formaldehyde catalytic oxidation. Chem Eng J 385:123887. https://doi.org/10.1016/j.cej.2019.123887

Chen F, Liu S, Yu J (2016) Efficient removal of gaseous formaldehyde in air using hierarchical titanate nanospheres with in situ amine functionalization. Phys Chem Chem Phys 18:18161–18168. https://doi.org/10.1039/C6CP03037H

Chen M, Wang H, Chen X, Wang F, Qin X, Zhang C, He H (2020b) High-performance of $Cu\text{-}TiO_2$ for photocatalytic oxidation of formaldehyde under visible light and the mechanism study. Chem Eng J 390:124481. https://doi.org/10.1016/j.cej.2020.124481

Chiang CY, Liu YY, Chen YS, Liu HS (2012) Absorption of hydrophobic volatile organic compounds by a rotating packed bed. Ind Eng Chem Res 51(27):9441–9445. https://doi.org/10.1021/ie2021637

Chiang YC, Chiang PC, Huang CP (2001) Effects of pore structure and temperature on VOC adsorption on activated carbon. Carbon 4(39):523–534. https://doi.org/10.1016/S0008-6223(00)00161-5

Chu L, Deng S, Zhao R, Zhang Z, Li C, Kang X (2015) Adsorption/desorption performance of volatile organic compounds on electrospun nanofibers. RSC Adv 5(124):102625–102632. https://doi.org/10.1039/C5RA22597C

Cui F, Han W, Si Y, Chen W, Zhang M, Kim HY, Ding B (2019) In situ synthesis of $MnO_2@SiO_2–TiO_2$ nanofibrous membranes for room temperature degradation of formaldehyde. Compos Commun 16:61–66. https://doi.org/10.1016/j.coco.2019.08.002

Deng S, Sourirajan A, Matsuura T, Farnand B (1995) Study of Volatile Hydrocarbon Emission Control by an Aromatic Poly(ether imide) Membrane. Ind Eng Chem Res 34(12):4494–4500. https://doi.org/10.1021/ie00039a041

Ding J, Rui Z, Lyu P, Liu Y, Liu X, Ji H (2018) Enhanced formaldehyde oxidation performance over Pt/ZSM-5 through a facile nickel cation modification. Appl Surf Sci 457:670–675. https://doi.org/10.1016/j.apsusc.2018.06.302

Dwivedi P, Gaur V, Sharma A, Verma N (2004) Comparative study of removal of volatile organic compounds by cryogenic condensation and adsorption by activated carbon fiber. Sep Purif Technol 39(1–2):23–37. https://doi.org/10.1016/j.seppur.2003.12.016

Fahri F, Bacha K, Chiki FF, Mbakidi JP, Panda S, Bouquillon S, Fourmentin S (2020) Environ Chem Lett 18:1403–1411. https://doi.org/10.1007/s10311-020-01007-8

Gard S (1957) Inactivation of poliovirus by formaldehyde: theoretical and practical aspects. Bull World Health Organ 17(6):979–989 (**PMID: 13511143; PMCID: PMC2537623**)

Ge JC, Kim JH, Choi NJ (2016) Electrospun polyurethane/loess powder hybrids and their absorption of volatile organic compounds. Adv Mater Sci Eng 2016:1–8. https://doi.org/10.1155/2016/8521259

Gesser HD, Fu S (1990) Removal of aldehydes and acidic pollutants from indoor air. Environ Sci Technol 24(4):495–497. https://doi.org/10.1021/es00074a005

Gopinath A, Kadirvelu K (2018) Strategies to design modified activated carbon fibers for the decontamination of water and air. Environ Chem Lett 16:1137–1168. https://doi.org/10.1007/s10311-018-0740-9

Gopinath KP, Vo DVN, Prakash DG, Joseph AA, Viswanathan S, Arun J (2020) Environmental applications of carbon-based materials: a review. Environ Chem Lett. https://doi.org/10.1007/s10311-020-01084-9

Guieysse B, Hort C, Platel V, Munoz R, Ondarts M, Revah S (2008) Biological treatment of indoor air for VOC removal: potential and challenges. Biotechnol Adv 26(5):398–410. https://doi.org/10.1016/j.biotechadv.2008.03.005

Guillerm M, Couvert A, Amrane A, Norrant E, Breton A, Dumont E (2017) Toluene degradation by a water/silicone oil mixture for the design of two phase partitioning bioreactors. Chin J Chem Eng 25(10):1512–1518. https://doi.org/10.1016/j.cjche.2017.01.010

Guo J, Lin C, Jiang C, Zhang P (2019) Review on noble metal-based catalysts for formaldehyde oxidation at room temperature. Appl Surf Sci 475:237–255. https://doi.org/10.1016/j.apsusc.2018.12.238

Han KT, Ruan LW (2020) Effects of indoor plants on air quality: a systematic review. Environ Sci Pollut Res 27:16019–16051. https://doi.org/10.1007/s11356-020-08174-9

He FG, Du B, Sharma G, Stadler FJ (2019) Highly efficient polydopamine-coated poly(methyl methacrylate) nanofiber supported platinum–nickel bimetallic catalyst for formaldehyde oxidation at room temperature. Polymers 11(4):674. https://doi.org/10.3390/polym11040674

Heymes F, Manno-Demoustier P, Charbit F, Fanlo JL, Moulin P (2006) A new efficient absorption liquid to treat exhaust air loaded with toluene. Chem Eng J 115(3):225–231. https://doi.org/10.1016/j.cej.2005.10.011

Huang Q, Hu Y, Pei Y, Zhang J, Fu M (2019) In situ synthesis of TiO_2@NH_2-MIL-125 composites for use in combined adsorption and photocatalytic degradation of formaldehyde. Appl Catal B Environ 259:118106. https://doi.org/10.1016/j.apcatb.2019.118106

Huang Q, Lu Y, Si H, Yang B, Tao T, Zhao Y, Chen M (2018a) Study of complete oxidation of formaldehyde over MnOx–CeO2 mixed oxide catalysts at ambient temperature. Catal Lett 148:2880–2890. https://doi.org/10.1007/s10562-018-2479-0

Huang Q, Wang Q, TaoT ZY, Wang P, Ding Z, Chen M (2018b) Controlled synthesis of Bi_2O_3/TiO_2 catalysts with mixed alcohols for the photocatalytic oxidation of HCHO. Environ Technol 40(15):1937–1947. https://doi.org/10.1080/09593330.2018.1432700

Huang Y, Ye K, Li H, Fan W, Zhao F, Zhang Y, Ji H (2016) A highly durable catalyst based on Co_xMn_3–xO_4 nanosheets for low-temperature formaldehyde oxidation. Nano Res 9:3881–3892. https://doi.org/10.1007/s12274-016-1257-9

Hu M, Yin L, Zhou H, Wu L, Yuan K, Pan B, Zhong Z, Xing W (2020) Manganese dioxide-filled hierarchical porous nanofiber membrane for indoor air cleaning at room temperature. J Membr Sci 605:118094. https://doi.org/10.1016/j.memsci.2020.118094

Ibhadon AO, Fitzpatrick P (2013) Heterogeneous photocatalysis: recent advances and applications. Catalysts 3(1):189–218. https://doi.org/10.3390/catal3010189

Indarto A, Choi JW, Lee H, Song HK (2008) Decomposition of greenhouse gases by plasma. Environ Chem Lett 6:215–222. https://doi.org/10.1007/s10311-008-0160-3

Jang KS, Kim HJ, Johnson JR, Kim W, Koros WJ, Jones CW, Nair S (2011) Modified mesoporous silica gas separation membranes on polymeric hollow fibers. Chem Mater 23(12):3025–3028. https://doi.org/10.1021/cm200939d

Jiun-Horng T, Hsiu-Mei C, Guan-Yinag H, Hung-Lung C (2008) Adsorption characteristics of acetone, chloroform and acetonitrile on sludge-derived adsorbent, commercial granular activated carbon and activated carbon fibers. J Hazard Mater 1–3(154):1183–1191. https://doi.org/10.1016/j.jhazmat.2007.11.065

Kadam V, Truong YB, Easton CD, Mukherjee S, Wang L, Padhye R, Kyratzis IL (2018) Electrospun polyacrylonitrile/β-cyclodextrin composite membranes for simultaneous air filtration and adsorption of volatile organic compounds. ACS Appl Nano Mater 1(8):4268–4277. https://doi.org/10.1021/acsanm.8b01056

Kadam V, Truong YB, Schutz J, Kyratzis IL, Padhye R, Wang L (2020) Gelatin/β–cyclodextrin bio-nanofibers as respiratory filter media for filtration of aerosols and volatile organic compounds at low air resistance. J Hazard Mater 403:123841. https://doi.org/10.1016/j.jhazmat.2020.123841

Kamal MS, Razzak SA, Hossain MM (2016) Catalytic oxidation of volatile organic compounds (VOCs) — a review. Atmos Environ 140:117–134. https://doi.org/10.1016/j.atmosenv.2016.05.031

Katepalli H, Bikshapathi M, Sharma CS, Verma N, Sharma A (2011) Synthesis of hierarchical fabrics by electrospinning of PAN nanofibers on activated carbon microfibers for environmental remediation applications. Chem Eng J 171(3):1194–1200. https://doi.org/10.1016/j.cej.2011.05.025

Kayaci F, Uyar T (2014) Electrospun polyester/cyclodextrin nanofibers for entrapment of volatile organic compounds. Polym Eng Sci 54(12):2970–2978. https://doi.org/10.1002/pen.23858

Kebede MA, Imae T, Sabrina WuCM, Cheng KB (2017) Cellulose fibers functionalized by metal nanoparticles stabilized in dendrimer for formaldehyde decomposition and antimicrobial activity. Chem Eng J 311:340–347. https://doi.org/10.1016/j.cej.2016.11.107

Kelly TJ, Dl S, Satola J (1999) Emission rates of formaldehyde from materials and consumer products found in California homes. Environ Sci Technol 33(1):81–88. https://doi.org/10.1021/es980592+

Khan FI, Ghoshal AK (2000) Removal of volatile organic compounds from polluted air. J Loss Prev Process Ind 13(6):527–545. https://doi.org/10.1016/S0950-4230(00)00007-3

Kim D, Park JH, Kim SD, Lee JY, Yim JH, Jeon JK, Park SH, Park YK (2011) Comparison of removal ability of indoor formaldehyde over different materials functionalized with various amine groups. J Ind Eng Chem 17(1):1–5. https://doi.org/10.1016/j.jiec.2010.12.010

Kim KJ, Jeong MI, Lee DW, Song JS, Kim HD, Yoo EH, Jeong SJ, han SW (2010) Variation in formaldehyde removal efficiency among indoor plant species. Hortscience 45(10):1489–1495. https://doi.org/10.21273/HORTSCI.45.10.1489

Klauson D, Portjanskaja E, Preis S (2008) Visible light-assisted photocatalytic oxidation of organic pollutants using nitrogen-doped Titania. Environ Chem Lett 6:35–39. https://doi.org/10.1007/s10311-007-0109-y

Kong J, Yee WA, Wei Y, Yang L, Ang JM, Phua SL, Wong SY, Zhou R, Dong Y, Li X, Lu X (2013) Silicon nanoparticles encapsulated in hollow graphitized carbon nanofibers for lithium ion battery anodes. Nanoscale 5(7):2967–2973. https://doi.org/10.1039/C3NR34024D

Kumar A, Thakur PR, Sharma G, Naushad M, Rana MGT, Stadler FJ (2019) Carbon nitride, metal nitrides, phosphides, chalcogenides, perovskites and carbides nanophotocatalysts for environmental applications. Environ Chem Lett 17:655–682. https://doi.org/10.1007/s10311-018-0814-8

Lee JH, Doan TA, Park YJ, Hoa HTM, Phuong PH, Le DT, Hung NH, Tran QT, Lee HS, Ryu JH, Yoo JY, Cuong TV (2020) Synthesis and photocatalytic activity of β-Ga2O3 nanostructures for decomposition of formaldehyde under deep ultraviolet irradiation. Catalysts 10(10):1105. https://doi.org/10.3390/catal10101105

Lee K, Choi JH, Lee S, Park HJ, Oh YJ, Kim GB, Lee W, Son B (2018) Indoor levels of volatile organic compounds and formaldehyde from emission sources at elderly care centers in Korea. PLoS ONE 13(6):e0197495. https://doi.org/10.1371/journal.pone.0197495

Lee KJ, Shiratori N, Lee GH, Miyawaki J, Mochida I, Yoon SH, Jang J (2010) Activated carbon nanofiber produced from electrospun

polyacrylonitrile nanofiber as a highly efficient formaldehyde adsorbent. Carbon 48(15):4248–4255. https://doi.org/10.1016/j.carbon.2010.07.034

Leson G, Winer AM (1991) Biofiltration: an innovative air pollution control technology for VOC emissions. J Air Waste Manag Assoc 41(8):1045–1054. https://doi.org/10.1080/10473289.1991.10466898

Levine LH, Richards JT, Coutts JL, Soler R, Maxik F, Wheeler RM (2011) Feasibility of ultraviolet-light-emitting diodes as an alternative light source for photocatalysis. J Air Waste Manag Assoc 61(9):932–940. https://doi.org/10.1080/10473289.2011.596746

Le Y, Guo D, Cheng B, Yu J (2013) Bio-template-assisted synthesis of hierarchically hollow SiO_2 microtubes and their enhanced formaldehyde adsorption performance. Appl Surf Sci 274:110–116. https://doi.org/10.1016/j.apsusc.2013.02.123

Lia XS, Maa XY, Liua JL, Suna ZG, Zhub B, Zhu AM (2019) Plasma-promoted Au/TiO2 nanocatalysts for photocatalytic formaldehyde oxidation under visible-light irradiation. Catal Today 337:132–138. https://doi.org/10.1016/j.cattod.2019.03.033

Li K, Ji J, Huang H, He M (2019a) Efficient activation of Pd/CeO2 catalyst by non-thermal plasma for complete oxidation of indoor formaldehyde at room temperature. Chemosphere 246:125762. https://doi.org/10.1016/j.chemosphere.2019.125762

Li Y, Abedalwafa MA, Tang L, Li D, Wang L (2019b) Electrospun Nanofibers for Sensors. In: Electrospinning: Nanofabrication and Applications, pp 571–601. https://doi.org/https://doi.org/10.1016/B978-0-323-51270-1.00018-2

Li L, Ma X, Chen R, Wang C, Lu M (2018) Nitrogen-containing functional groups-facilitated acetone adsorption by ZIF-8-derived porous carbon. Materials 11(1):159. https://doi.org/10.3390/ma11010159

Lin L, Chai Y, Zhao B, Wei W, He D, He B, Tang Q (2012) Photocatalytic oxidation for degradation of VOCs. Open J Inorg Chem 3(1):14–25. https://doi.org/10.4236/ojic.2013.31003

Liu D, Li B, Wu J, Liu Y (2020a) Photocatalytic oxidation removal of elemental mercury from flue gas. A review. Environ Chem Lett 18:417–431. https://doi.org/10.1007/s10311-019-00957-y

Liu F, Chen Y, Shao W, Yue W, Li M, Liao X, Weng K, Li F, Ni QQ, Wang L, He J (2020b) Preparation of polystyrene nanofiber-supported metal-organic framework with formaldehyde adsorption properties. J Fiber Sci Technol 76(1):43–49. https://doi.org/10.2115/fiberst.2020-0005

Liu H, Ye X, Lian Z, Wen Y, Shangguan W (2006) Experimental study of photocatalytic oxidation of formaldehyde and its by-products. Res Chem Intermed 32(1):9–16. https://doi.org/10.1163/156856706775012978

Liu Y, Jia H, Li C, Sun Z, Pan Y, Zheng S (2019) Efficient removal of gaseous formaldehyde by amine-modified diatomite: a combined experimental and density functional theory study. Environ Sci Pollut Res 26:25130–25141. https://doi.org/10.1007/s11356-019-05758-y

Liu Z, Niu J, Long W, Cui B, Song K, Dong F, Xu D (2020c) Highly efficient MnO_2/AlOOH composite catalyst for indoor low- concentration formaldehyde removal at room temperature. Inorg Chem 59(10):7335–7343. https://doi.org/10.1021/acs.inorgchem.0c00852

Llanos J, Vercik L, Vercik A (2015) Physical properties of Chitosan films obtained after neutralization of polycation by slow drip method. J Biomater Nanobiotechnol 6(4):276–291. https://doi.org/10.4236/jbnb.2015.64026

Louangsouphom B, Wang X, Song J, Wang X (2019) Low-temperature preparation of a N-TiO2/macroporous resin photocatalyst to degrade organic pollutants. Environ Chem Lett 17:1061–1066. https://doi.org/10.1007/s10311-018-00827-z

Lu L, Tian H, He J, Yang Q (2016) Graphene−MnO_2 hybrid nanostructure as a new catalyst for formaldehyde oxidation. J Phys Chem C 120(41):23660–23668. https://doi.org/10.1021/acs.jpcc.6b08312

Luna MDG, Laciste MT, Tolosa NC, Lu MC (2018) Effect of catalyst calcination temperature in the visible light photocatalytic oxidation of gaseous formaldehyde by multi-element doped titanium dioxide. Environ Sci Pollut Res 25:15216–15225. https://doi.org/10.1007/s11356-018-1720-0

Lu Y, Wang D, Ma C, Yang H (2010) The effect of activated carbon adsorption on the photocatalytic removal of formaldehyde. Build Environ 45(3):615–621. https://doi.org/10.1016/j.buildenv.2009.07.019

Lu Y, Wang D, Wu Y, Ma C, Zhang X, Yang C (2012) Synergistic effect of nanophotocatalysis and nonthermal plasma on the removal of indoor HCHO. Int J Photoenergy 2012:1–8. https://doi.org/10.1155/2012/354032

Ma C, Li X, Zhu T (2011) Removal of low-concentration formaldehyde in air by adsorption on activated carbon modified by hexamethylene diamine. Carbon 49(8):2869–2877. https://doi.org/10.1016/j.carbon.2011.02.058

Madhura L, Kanchi S, Sabela MI, Singh S, Bisetty K, Inamuddin (2018) Membrane technology for water purification. Environ Chem Lett 16:343–365. https://doi.org/10.1007/s10311-017-0699-y

Mamaghani AH, Haghighat F, Lee CS (2017) Photocatalytic oxidation technology for indoor environment air purification: the state-of-the-art. Appl Catal B Environ 203:247–269. https://doi.org/10.1016/j.apcatb.2016.10.037

Ma Y, Zhang G (2016) Sepiolite nanofiber-supported platinum nanoparticle catalysts toward the catalytic oxidation of formaldehyde at ambient temperature: efficient and stable performance and mechanism. Chem Eng J 288:70–78. https://doi.org/10.1016/j.cej.2015.11.077

Miao L, Wang J, Zhang P (2019) Review on manganese dioxide for catalytic oxidation of airborne formaldehyde. Appl Surf Sci 466:441–453. https://doi.org/10.1016/j.apsusc.2018.10.031

Mughal MJ, Saeed R, Naeem M, Ahmed AM, Yasmien A, Siddiqui Q, Iqbal M (2013) Dye fixation and decolourization of vinyl sulphone reactive dyes by using dicyanidiamide fixer in the presence of ferric chloride. J Saudi Chem Soc 17(1):23–28. https://doi.org/10.1016/j.jscs.2011.02.017

Na CJ, Yoo MJ, Tsang DCW, Kim HW, Kim KH (2018) High-performance materials for effective sorptive removal of formaldehyde in air. J Hazard Mater 366:452–465. https://doi.org/10.1016/j.jhazmat.2018.12.011

Nallathambi G, Berly R, Esmeralda SP, Kumaravel J, Parthiban V (2019) Development of SPI/AC/PVA nano-composite for air-filtration and purification. Res J Text Appar 24(1):72–83. https://doi.org/10.1108/RJTA-09-2019-0044

Nallathambi G, Vijayalakshmi E, Berly R, Srinivasan NR (2018) Development of PAN nano fibrous filter hybridized by SiO_2 nanoparticles electret for high efficiency air filtration. J Polym Mater 35(3):309–320. https://doi.org/10.32381/JPM.2018.35.03.6

Nie L, Yu J, Fu J (2014) Complete decomposition of formaldehyde at room temperature over a Platinum-decorated hierarchically porous electrospun titania nanofiber mat. ChemCatChem 6(7):1983–1989. https://doi.org/10.1002/cctc.201301105

Nomura A, Jones CW (2013) Amine-functionalized porous silicas as adsorbents for aldehyde abatement. ACS Appl Mater Interfaces 5(12):5569–5577. https://doi.org/10.1021/am400810s

Nuasaen S, Opaprakasit P, Tangboriboonrat P (2013) Hollow latex particles functionalized with chitosan for the removal of formaldehyde from indoor air. Carbohydr Polym 101:179–187. https://doi.org/10.1016/j.carbpol.2013.09.059

Pan B, Xing B (2008) Adsorption mechanisms of organic chemicals on carbon nanotubes. Environ Sci Technol 42(24):9005–9013. https://doi.org/10.1021/es801777n

Pei J, Zhang JS (2010) On the performance and mechanisms of formaldehyde removal by chemi-sorbents. Chem Eng J 167(1):59–66. https://doi.org/10.1016/j.cej.2010.11.106

Pei J, Zhang JS (2011) Critical review of catalytic oxidization and chemisorption methods for indoor formaldehyde removal. HVAC R Res 17(4):476–503. https://doi.org/10.1080/10789669.2011.587587

Photong S, Boonamnuayvitaya V (2009) Enhancement of formaldehyde degradation by amine functionalized silica/titania films. J Environ Sci 21(12):1741–1746. https://doi.org/10.1016/S1001-0742(08)62482-1

Quiroz J, Giraudon MJ, Gervasini A, Dujardin C, Lancelot C, Trentesaux M, Lamonier JF (2015) Total oxidation of formaldehyde over MnO_x-CeO_2 catalysts: the effect of acid treatment. ACS Catal 5(4):2260–2269. https://doi.org/10.1021/cs501879j

Rengga WDP, Sudibandriyo M, Nasikin M (2013) Adsorption of low-concentration formaldehyde from air by silver and copper nano-particles attached on bamboo-based activated carbon. Int J Chem Eng Appl 4(5):332–336. https://doi.org/10.7763/IJCEA.2013.V4.320

Ren X, Chen C, Nagatsu M, Wang X (2010) Carbon nanotubes as adsorbents in environmental pollution management: a review. Chem Eng J 170:395–410. https://doi.org/10.1016/j.cej.2010.08.045

Ren L, Yu Y, Yang Y, Zhang Q, Xiao X, Liu R, Xu W (2020) Efficient removal of formaldehyde with ZIF-8 growth on TiO_2-coated activated carbon fiber felts prepared via atomic layer deposition. J Mater Sci 55:3167–3180. https://doi.org/10.1007/s10853-019-04142-y

Rethinam S, Berly R, Ram TB, Nallathambi G (2018) Electrospun poly(vinyl) alcohol/collagen nanofibrous scaffold hybridized by graphene oxide for accelerated wound healing. Int J Artif Organs 41(8):467–473. https://doi.org/10.1177/0391398818775949

Rezaee A, Rangkooy H, Jonidi-Jafari A, Khavanin A (2013) Surface modification of bone char for removal of formaldehyde from air. Appl Surf Sci 286:235–239. https://doi.org/10.1016/j.apsusc.2013.09.053

Rezaee A, Rangkooy H, Khavanin A, Jafari AJ (2014) High photocatalytic decomposition of the air pollutant formaldehyde using nano-ZnO on bone char. Environ Chem Lett 12:353–357. https://doi.org/10.1007/s10311-014-0453-7

Rong H, Ryu Z, Zheng J, Zhang Y (2003) Influence of heat treatment of rayon-based activated carbon fibers on the adsorption of formaldehyde. J Colloid Interf Sci 261:207–212. https://doi.org/10.1016/S0021-9797(03)00099-7

Saeung S, Boonamnuayvitaya V (2007) Adsorption of formaldehyde vapor by amine-functionalized mesoporous silica materials. J Environ Sci 20(3):379–384. https://doi.org/10.1016/S1001-0742(08)60059-5

Saleem J, Shahid UB, Hijab M, Mackey H, McKay G (2019) Production and applications of activated carbons as adsorbents from olive stones. Biomass Convers Biorefin 9:775–802. https://doi.org/10.1007/s13399-019-00473-7

Salthammer T, Mentese S, Marutzky R (2010) Formaldehyde in the indoor environment. Chem Rev 110(4):2536–2572. https://doi.org/10.1021/cr800399g

Sargazi G, Afzali D, Mostafavi A, Shadman A, Rezaee B, Zarrintaj P, Saeb MR, Ramakrishna S, Mozafari M (2019) Chitosan/polyvinyl alcohol nanofibrous membranes: towards green super-adsorbents for toxic gases. Heliyon 5(4):e01527. https://doi.org/10.1016/j.heliyon.2019.e01527

Scholten E, Bromberg L, Rutledge GC, Hatton TA (2011) Electrospun polyurethane fibers for absorption of volatile organic compounds from air. ACS Appl Mater Interfaces 3(10):3902–3909. https://doi.org/10.1021/am200748y

Selvam AK, Nallathambi G (2015) Mesoporous $MgAl_2O_4$ and $MgTiO_3$ nanoparticles modified polyacrylonitrile nanofibres for 2-chloroethyl ethyl sulfide degradation. Fibers Polym 16(10):2121–2129. https://doi.org/10.1007/s12221-015-5429-0

Shah KW, Li W (2019) A review on catalytic nanomaterials for volatile organic compounds VOC removal and their applications for healthy buildings. Nanomater 9(6):910. https://doi.org/10.3390/nano9060910

Shalbafan A, Hassannejad H, Rahmaninia M (2020) Formaldehyde adsorption capacity of chitosan derivatives as bio-adsorbents for wood-based panels. Int J Adhes Adhes 102:102669. https://doi.org/10.1016/j.ijadhadh.2020.102669

Shie JL, Lee CH, Chiou CS, Chang CT, Chang CC, Chang CY (2008) Photodegradation kinetics of formaldehyde using light sources of UVA, UVC and UVLED in the presence of composed silver titanium oxide photocatalyst. J Hazard Mater 155(1–2):164–172. https://doi.org/10.1016/j.jhazmat.2007.11.043

Shih Y, Li M (2008) Adsorption of selected volatile organic vapors on multiwall carbon nanotubes. J Hazard Mater 154:21–28. https://doi.org/10.1016/j.jhazmat.2007.09.095

Song Y, Qiao W, Yoon SH, Mochida I, Guo Q, Liu L (2007) Removal of formaldehyde at low concentration using various activated carbon fibers. J Appl Polym Sci 106(4):2151–2157. https://doi.org/10.1002/app.26368

Souzandeh H, Johnson JS, Wang Y, Bhamidipaty K, Zhong WH (2016) Soy-protein-based nanofabrics for highly efficient and multifunctional air filtration. ACS Appl Mater Interfaces 8(31):20023–20031. https://doi.org/10.1021/acsami.6b05339

Souzandeh H, Wang Y, Zhong WHK (2013) "Green" nano-filters: fine nanofibers of natural protein for high efficiency filtration of particulate pollutants and toxic gases. RSC Adv 6(107):105948–105956. https://doi.org/10.1039/C6RA24512A

Speight JG (2019) 7 - Process classification. In: Speight JG (ed) Natural gas, 2nd edn. Gulf Professional Publishing, pp 219–276. https://doi.org/10.1016/B978-0-12-809570-6.00007-2

Sultana S, Vandenbroucke AM, Leys C, Geyter ND, Morent R (2015) Abatement of VOCs with alternate adsorption and plasma-assisted regeneration: a review. Catalysts 5(2):718–746. https://doi.org/10.3390/catal5020718

Sun S, Ding J, Bao J, Gao C, Qi Z, Li C (2010) Photocatalytic oxidation of gaseous formaldehyde on TiO2: an in situ DRIFTS study. Catal Lett 137:239–246. https://doi.org/10.1007/s10562-010-0358-4

Suresh S, Bandosz TJ (2018) Removal of formaldehyde on carbon -based materials: a review of the recent approaches and findings. Carbon 137:207–221. https://doi.org/10.1016/j.carbon.2018.05.023

Su Y, Ji K, Xun J, Zhang K, Liu P, Zhao L (2020) Catalytic oxidation of low concentration formaldehyde over Pt/TiO2 catalyst. Chin J Chem Eng. https://doi.org/10.1016/j.cjche.2020.04.024

Talaiekhozani A, Rezania S, Kim KH, Sanaye R, Amani AM (2020) Recent advances in photocatalytic removal of organic and inorganic pollutants in air. J Clean Prod 278:123895. https://doi.org/10.1016/j.jclepro.2020.123895

Tang B, Dai Y, Sun Y, Chen H, Wang Z (2020) Graphene and MOFs co-modified composites for high adsorption capacity and photocatalytic performance to remove pollutant under both UV- and visible-light irradiation. J Solid State Chem 284:121215. https://doi.org/10.1016/j.jssc.2020.121215

Torres JQ, Royer S, Bellat JP, Giraudon JM, Lamonier JF (2013) Formaldehyde: catalytic oxidation as a promising soft way of elimination. Chemsuschem 6:578–592. https://doi.org/10.1002/cssc.201200809

Uyar T, Havelund R, Nur Y, Balan A, Hacaloglu J, Toppare L, Besenbacher F, Kingshott P (2010) Cyclodextrin functionalized poly(methyl methacrylate) (PMMA) electrospun nanofibers for organic vapors waste treatment. J Membr Sci 365(1–2):409–417. https://doi.org/10.1016/j.memsci.2010.09.037

Vikrant K, Lim DH, Younis SA, Kim KH (2020) An efficient strategy for the enhancement of adsorptivity of microporous carbons against gaseous formaldehyde: surface modification with aminosilane adducts. Sci Total Environ 743:140761. https://doi.org/10.1016/j.scitotenv.2020.140761

Vikrant K, Qu Y, Kim K, Bukhvalov D, Ah W (2020) Amine-functionalized microporous covalent organic polymers for adsorptive removal of a gaseous aliphatic aldehyde mixture. Environ Sci Nano. https://doi.org/10.1039/D0EN00537A

Wang J, Zhang P, Li J, Jiang C, Yunus R, Kim J (2015) Room-temperature oxidation of formaldehyde by layered manganese oxide: effect of water. Environ Sci Technol 49(20):12372–12379. https://doi.org/10.1021/acs.est.5b02085

Wang SX, Yang L, Stubbs LP, Li X, He C (2013) Lignin-derived fused electrospun carbon fibrous mats as high performance anode materials for lithium ion batteries. ACS Appl Mater Interfaces 5(23):12275–12282. https://doi.org/10.1021/am4043867

Wang T, Wang Y, Sun M, Hanif A, Wu H, Gu Q, Ok YS, Tsang DCW, Li J, Yu J, Shang J (2020) Thermally treated zeolitic imidazolate framework- 8 (ZIF-8) for visible light photocatalytic degradation of gaseous formaldehyde. Chem Sci 11(26):6670. https://doi.org/10.1039/D0SC01397H

Wang X, Yu J, Sun G, Ding B (2015) Electrospun nanofibrous materials: a versatile medium for effective oil/water separation. Mater Today 19(7):403–414. https://doi.org/10.1016/j.mattod.2015.11.010

Wang Z, Chen B, Crocker M, Yu L, Shi C (2020) New insights into alkaline metal modified CoMn-oxide catalysts for formaldehyde oxidation at low temperatures. Appl Catal A Gen 592:117512. https://doi.org/10.1016/j.apcata.2020.117512

Wen Q, Li C, Cai Z, Zhang W, Gao H, Chen L, Zeng G, Shu X, Zhao Y (2010) Study on activated carbon derived from sewage sludge for adsorption of gaseous formaldehyde. Bioresour Technol 102(2011):942–947. https://doi.org/10.1016/j.biortech.2010.09.042

Wen Y, Tang X, Li J, Hao J, Wei L, Tang X (2009) Impact of synthesis method on catalytic performance of MnO_x–SnO_2 for controlling formaldehyde emission. Catal Commun 10(8):1157–1160. https://doi.org/10.1016/j.catcom.2008.12.033

Wua J, Yia H, Tanga X, Zhaoa S, Xua J, Meng J, Li Q (2020) Catalytic oxidation of formaldehyde by MnCo3MOx catalyst: effect of rare earth elements and temperature. Mater Chem Phys 240:122123. https://doi.org/10.1016/j.matchemphys.2019.122123

Wu L, Qin Z, Zhang L, Meng T, Yu F, Ma J (2017) CNT-enhanced amino-functionalized graphene aerogel adsorbent for highly efficient removal of formaldehyde. New J Chem 41(7):2527–2533. https://doi.org/10.1039/C6NJ03643K

Wu L, Zhang L, Meng T, Yu F, Chen J, Ma J (2015) Facile synthesis of 3D amino-functional graphene-sponge composites decorated by graphene nanodots with enhanced removal of indoor formaldehyde. Aerosol Air Qual Res 15:1028–1034. https://doi.org/10.4209/aaqr.2014.10.0237

Wu Y, Song M, Chai Z, Huang J, Wang X (2020) Facile construction of bi_2moo_6/bi/g-c_3n_4 toward efficient photocatalytic oxidation of indoor gaseous formaldehyde with a wide concentration range under visible light irradiation. ACS Sustain Chem Eng 8(20):7710–7720. https://doi.org/10.1021/acssuschemeng.0c01630

Xu J, Qu Z, Wang Y, Huang B (2018) HCHO oxidation over highly dispersed Au nanoparticles supported on mesoporous silica with superior activity and stability. Catal Today 327:210–219. https://doi.org/10.1016/j.cattod.2018.04.051

Yamanaka S, Suzuma A, Fujimoto T, Kuga Y (2013) Production of scallop shell nanoparticles by mechanical grinding as a formaldehyde adsorbent. J Nanopart Res 15:1573. https://doi.org/10.1007/s11051-013-1573-x

Yang KH, Liu YC, Yu CC, Chen BC (2011) Fabrication of chitosan/silver nanocomposites based on electrochemical methods for removing formaldehyde in air. Mater Chem Phys 126(3):993–997. https://doi.org/10.1016/j.matchemphys.2010.09.069

Yang S, Zhu Z, Wei F, Yang X (2017) Enhancement of formaldehyde removal by activated carbon fiber via in situ growth of carbon nanotubes. Build Environ 126:27–33. https://doi.org/10.1016/j.buildenv.2017.09.025

Yang X, Wan Y, Zheng Y, He F, Yu Z, Huang J, Wang H, Ok YS, Jiang Y, Gao B (2019) Surface functional groups of carbon-based adsorbents and their roles in the removal of heavy metals from aqueous solutions: a critical review. Chem Eng J 366:608–621. https://doi.org/10.1016/j.cej.2019.02.119

Yang Y, Su Y, Zhao S (2020) An efficient plant–microbe phytoremediation method to remove formaldehyde from air. Environ Chem Lett 18:197–206. https://doi.org/10.1007/s10311-019-00922-9

Yang Z, Miao H, Rui Z, Ji H (2019) Enhanced formaldehyde removal from air using fully biodegradable chitosan grafted -cyclodextrin adsorbent with weak chemical interaction. Polymers 11(2):276. https://doi.org/10.3390/polym11020276

Ye J, Zhou M, Le Y, Cheng B, Yu J (2020) Three-dimensional carbon foam supported MnO2/Pt for rapid capture and catalytic oxidation of formaldehyde at room temperature. Appl Catal B 267:118689. https://doi.org/10.1016/j.apcatb.2020.118689

Ye J, Zhu X, Cheng B, Yu J, Jiang C (2016) Few-layered graphene-like boron nitride: a highly efficient adsorbent for indoor formaldehyde removal. Environ Sci Technol Lett 4(1):20–25. https://doi.org/10.1021/acs.estlett.6b00426

Yi Y, Li C, Zhao L, Du X, Gao L, Chen J, Zhai Y, Zeng G (2018) The synthetic evaluation of CuO-MnO_x-modified pinecone biochar for simultaneous removal formaldehyde and elemental mercury from simulated flue gas. Environ Sci Pollut Res 25:4761–4775. https://doi.org/10.1007/s11356-017-0855-8

Yu L, Wang L, Sun X, Ye D (2018) Enhanced photocatalytic activity of rGO/TiO for the decomposition of formaldehyde under visible light irradiation. J Environ Sci 73:138–146. https://doi.org/10.1016/j.jes.2018.01.022

Zhang C, Wang Y, Song W, Zhang H, Zhang X, Li R, Fan C (2020) Synthesis of MnO_2 modified porous carbon spheres by preoxidation-assisted impregnation for catalytic oxidation of indoor formaldehyde. J Porous Mater 27:801–815. https://doi.org/10.1007/s10934-020-00860-w

Zhang D, Zhang M, Ding F, Liu W, Zhang L, Cui L (2020) Efficient removal of formaldehyde by polyethyleneimine modified activated carbon in a fixed bed. Environ Sci Pollut Res 27:18109–18116. https://doi.org/10.1007/s11356-020-08019-5

Zhang J, Li Y, Wang L, Zhang C, He H (2015) Catalytic oxidation of formaldehyde over manganese oxides with different crystal structures. Catal Sci Technol 5(4):2305–2313. https://doi.org/10.1039/C4CY01461H

Zhang J, Yang P, Zheng J, Li J, Lv S, Jin T, Zou Y, Xu P, Cheng C, Zhang Y (2020) Degradation of gaseous HCHO in a rotating photocatalytic fuel cell system with an absorption efficiency of up to 94%. Chem Eng J 392:123634. https://doi.org/10.1016/j.cej.2019.123634

Zhang X, Gao B, Creamer AE, Cao C, Li Y (2017) Adsorption of VOCs onto engineered carbon materials: A review. J Hazard Mater 338:102–12. https://doi.org/10.1016/j.jhazmat.2017.05.013

Zheng Y, Wang W, Jiang D, Zhang L (2015) Amorphous MnO_x modified Co_3O_4 for formaldehyde oxidation: improved

low-temperature catalytic and photothermocatalytic activity. Chem Eng J 284:21–27. https://doi.org/10.1016/j.cej.2015.08.137

Zhou J, Qin J, Xiao W, Zeng C, Li N, Lv T, Zhu H (2017) Oriented growth of layered-MnO_2 nanosheets over α-MnO2 nanotubes for enhanced room-temperature HCHO oxidation. Appl Catal B Environ 207(15):233–243. https://doi.org/10.1016/j.apcatb.2017.01.083

Zhu J, Chen J, Zhuang P, Zhang Y, Wang Y, Tan H, Feng J, Yan W (2020) Efficient adsorption of trace formaldehyde by polyaniline/TiO_2 composite at room temperature and mechanism investigation. Atmos Pollut Res. https://doi.org/10.1016/j.apr.2020.09.015

Zhu Q, Tang X, Feng S, Zhong Z, Yao J, Yao Z (2019) ZIF-8@SiO_2 composite nanofiber membrane with bioinspired spider web- like structure for efficient air pollution control. J Membr Sci 581:252–261. https://doi.org/10.1016/j.memsci.2019.03.075

Zhu X, Gao X, Qin R, Zeng Y, Qu R, Zheng C, Tu X (2015) Plasma-catalytic removal of formaldehyde over Cu–Ce catalysts in a dielectric barrier discharge reactor. Appl Catal B Environ 170:293–300. https://doi.org/10.1016/j.apcatb.2015.01.032